Proceedings of CONF-MCEE 2026 Symposium: Advances in Sustainable Aviation and Aerospace Vehicle Automation
DOI: 10.54254/2755-2721/2026.KA29339

A Comprehensive Review of Non-Fluorinated Durable Water-Repellent and Stain-Resistant Coatings

Zicheng Tang[1*†], Yuerong Tian[2†], Chenyu Zhang[3†], Dechen Feng[4†]

[1]*Material and nanoscience, University of Waterloo, Waterloo, Canada*
[2]*BSc Honours in Chemistry, University of Bristol, Bristol, United Kingdom*
[3]*Shenghua Zizhu Academy, Shanghai, China*
[4]*Affiliated High School of South China Normal University, Guangzhou, China*
**Corresponding Author. Email: z24tang@uwaterloo.ca*
[†]*These authors contributed equally to this work and should be considered as co-first author.*

Abstract. For industries manufacturing textiles and functional surfaces that must resist water, stains, and environmental degradation, durable water-repellent (DWR) coatings are indispensable. Fluorinated DWRs have long dominated the market due to their excellent durability under adverse conditions and their combined hydrophobic, oleophobic, and stain-resistant properties. However, concerns over the toxicity of fluorinated compounds and harmful by-products generated during production and degradation have catalysed the search for sustainable, fluorine-free alternatives. This review begins with the fundamental principles of wettability, hydrophobicity, and stain resistance, drawing on classic theories, models, and biological inspirations such as lotus leaves, shark skin, insect ommatea, and spider silk. The discussion then shifts to non-fluorinated DWRs, organized by functional mechanism and fabrication strategy, with emphasis on the roles of surface energy reduction and surface roughness engineering. Four representative classes—hydrocarbon-based, silicon-containing, bio-derived, and nanoparticle-based coatings—are evaluated to assess the potential of current synthetic approaches in producing reliable and environmentally benign replacements. Finally, emerging applications across textiles and related hydrophobic materials are summarized, highlighting both the progress achieved and the challenges that remain for the development of next-generation sustainable DWRs.

Keywords: durable water repellent, non-fluorinated, hydrophobicity, stain-resistant, wetting

1. Introduction

1.1. Traditional fluorinated coating materials and their limitations

Traditional fluorinated coatings, mainly based on perfluoroalkyl and polyfluoroalkyl substances (PFAS), have been widely valued for their outstanding ability to repel water and oil. This key feature results from their unique molecular structure, which creates an extremely low surface energy. This allows the coatings to form a protective barrier on surfaces, effectively stopping water and oil from spreading or soaking in. Consequently, materials treated with these coatings maintain long-lasting

© 2025 The Authors. This is an open access article distributed under the terms of the Creative Commons Attribution License 4.0 (https://creativecommons.org/licenses/by/4.0/).

DOI: 10.54254/2755-2721/2026.KA29339

water resistance and stain protection [1]. Beyond this repellency, fluorinated coatings are also highly chemically stable. This stability ensures reliable performance even under demanding conditions, making them suitable for diverse applications. Combined with mature manufacturing techniques and dependable supply chains, traditional fluorinated coatings have historically been the leading choice for durable waterproof and stain-resistant solutions.

However, these materials possess significant and growing drawbacks. Environmentally, PFAS are highly persistent. They resist both chemical breakdown and natural biological processes, leading to their designation as "forever chemicals." They can remain in soil, groundwater, and the atmosphere for hundreds of years, accumulating through the food chain and eventually entering humans via consumption or air [2]. Numerous studies indicate that long-term PFAS exposure is associated with various health risks, including hormone disruption, weakened immunity, and higher rates of certain cancers [3]. Furthermore, the production of fluorinated coatings itself generates harmful waste products, adding to environmental damage. The pressure of environmental hazards has accelerated the search for sustainable alternatives. Nevertheless, a major hurdle persists: these alternatives must achieve performance levels comparable to fluorinated coatings, particularly in liquid repellency and durability, while also being environmentally safe and affordable for widespread use. This highlights the considerable urgency and complexity involved in shifting materials science towards more sustainable options.

1.2. Societal priorities and unresolved challenges

The shift in global environmental goals and cultural priorities is reflected in the trend towards non fluorinated waterproof and anti fouling coatings. In today's world, durable and effective waterproof and anti fouling coatings play a crucial role, with a wide range of applications - from daily necessities such as outdoor clothing and furniture, to industrial fields such as ship protection and food processing equipment. This type of coating not only prevents materials from being damaged by stains or water erosion, helps maintain their appearance, but more importantly, significantly extends their service life. In ship applications, they help prevent biological attachment; In the food industry, maintenance costs are reduced through more convenient cleaning processes. Therefore, people are now particularly concerned about its performance and environmental impact.

Growing awareness of sustainability has led both consumers and industries to prefer eco-friendly products, increasing demand for materials with lower ecological footprints. This trend is strengthened by the well-known environmental and health risks linked to traditional fluorinated coatings. Governments worldwide have reacted with stricter regulations. The tightening of global regulations, particularly bans and restrictions on many PFAS types in key regions such as the European Union and the United States, is significantly challenging the market dominance of traditional fluorinated coatings [4]. This combination of regulatory pressure and rising public concern about environmental health creates an urgent need to replace fluorinated materials with safer options.

Despite this progress, major challenges remain for the widespread use of non-fluorinated coatings. A key issue is matching the performance of fluorinated coatings. Current alternatives—such as certain silicone-based polymers, specially modified hydrocarbon waxes, or surfaces inspired by nature (like lotus leaves)—often fail to equal the outstanding liquid repellency of fluorinated versions. They frequently lose effectiveness after repeated washing, abrasion, or UV exposure. This is a serious drawback for demanding uses like outdoor apparel or industrial surfaces. Furthermore, scaling up production faces technical and economic hurdles. New manufacturing methods may need specialized equipment, and raw material costs can be higher than for fluorinated coatings, reducing

DOI: 10.54254/2755-2721/2026.KA29339

market competitiveness. These limitations highlight the need for focused research. Solutions must improve performance and ensure new coatings can be produced affordably on a large scale while remaining environmentally safe. Overcoming these obstacles remains a central challenge in materials science.

1.3. The definition of DWR coating and its market size and advantages

The scientific community's pursuit of fluorinated DWRs alternatives gained momentum after a landmark study in 2000 revealed the ubiquitous presence of perfluorooctanesulfonic acid (PFOS) in wildlife [5,6]. This finding reignited concerns regarding traditional fluorinated DWRs, whose organic fluorine compounds had been detected accumulating in human serum as early as the 1960s. The revelation of widespread environmental contamination due to the fluorine-containing substances produced during the process of either the manufacture of DWRs or the degradation of DWRs prompted urgent exploitation of persistent yet harmless waterproof coating materials [7-9].

Non-fluorinated DWR coatings are defined as surface treatment materials that maintain long-lasting water resistance without incorporating fluorinated compounds in their chemical composition. These DWR primarily encompass two categories: (1) perfluorinated non-octyl carbon compounds, namely side-chain fluorinated C6 and C4 polymers, which contain fluorine on their side chains only, (2) completely fluorine-free hydrophobic agents, including organosilicone derivatives and hydrocarbon-based macromolecular systems [10]. Current formulations typically integrate multiple polymeric architectures, including but not limited to polyurethane networks, functionalized nanoparticles, and hyper-branched dendritic structures [11-14].

Though the fluorine content in the alternatives, non-fluorinated DWRs, has been reduced, the overall technical performance and environmental friendliness are two prominent features of the new DWRs that are still somewhat untested [15].

For perfluorinated non-octyl carbon compounds, it is shorter fully fluorinated chains that endow C6 and C4 polymers with approximately the same liquid repellency as the traditional DWRs have. This is evident in the case of Hills' research in 2017, in which the trials were done on the outdoor apparel that was a spray treated non-fluorinated finishes. With reference to the BS ISO 23232:2009 and BS EN ISO 14419:2010 (standard assessment method for oil-repellency and water-repellency respectively), the results of all the spray-treated samples reflected a uniform and highly water-repellent finish. However, (C8) PFAS finished textiles were found to possess a far greater oleophobicity than other finished samples. Meanwhile, for the completely fluorine-free coatings, all saturated alkyl chains and polydimethylsiloxanes in the non-fluorinated DWRs demonstrated excellent liquid repellency just as those fluorine containing coatings did in the test [9]. Demand for waterproof clothing is on the rise, driven by a record 175.8 million participants in U.S. outdoor activities in 2023. This figure represents over half the American population aged six and older [15]. For people engaged in strenuous sports in remote, mountainous areas, the hydrophobicity of their sportswear is a crucial safety feature. When a garment's outer fabric gets wet, it can quickly become saturated, leading to evaporative cooling of perspiration. This process draws heat away from the body, affects the wearer's physiological responses, and can create a serious health and safety risk [16,17]. Recently, non-fluorinated DWRs have proven to be a successful solution for this mass market. They provide the necessary protection, keeping wearers dry and allowing the body to thermoregulate effectively, even in challenging weather [18-21].

Recent non-fluorinated DWRs are now being made with biodegradable materials. However, the byproducts of their breakdown—simple sugars, fatty acids, and silicone-modified saccharides—have not yet been fully studied to confirm they are safe for the environment. Despite this, these new

DOI: 10.54254/2755-2721/2026.KA29339

DWRs can still a greener option compared to older, persistent fluorinated DWRs like PFAS and PFCs. However, several unknowns still remain. For example, perfluorohexane sulfonate is increasingly being found in the environment and has a long half-life in mammals, similar to or longer than that of traditional DWRs [22].

1.4. Limitations of the existing non-fluorinated coating materials

Despite the growing demand for environmentally friendly alternatives, current non-fluorinated durable water repellents still have some significant limitations that hinder their widespread application and market acceptance. The most prominent problem is that they are not as effective as fluorinated materials at repelling water [23]. Although hydrocarbon-based non-fluorinated durable water repellents exhibit excellent water repellency, effectively resisting water penetration, with low water absorption and a small droplet roll-off angle (α roff-off = 22–23°), other non-fluorinated alternatives, such as silicon-based coatings (SiS), lack sufficient surface hydrophobicity to induce droplet roll-off, with higher water absorption (12–24 wt%), larger roll-off angles (α roff-off = 33–70°), or even no roll-off at all. This means that water can more easily penetrate the fabric structure, ultimately affecting the wearer's thermal comfort [23]. In addition, the performance of these coatings varies depending on their specific chemical formulations [24].

Another key limitation is the poor durability of these alternative coatings. They also have poor oil repellency, and oily liquids can easily penetrate the fabric [25]. Furthermore, non-fluorinated durable water-repellent coatings offer very poor stain resistance against high to medium surface tension liquids and no stain resistance at all against low surface tension liquids [26]. This means that garments treated with such coatings need to be frequently washed when exposed to oil or dirt [25]. Unfortunately, water repellents (e.g., silicone-based finishes) typically have only moderate resistance to washing and dry cleaning, and such coatings lose effectiveness quickly after repeated washings [25]. This significantly shortens the lifespan of treated garments, necessitating frequent replacement or reapplication of the coating.

Furthermore, even with the use of fluorine-free alternatives, environmental concerns remain. For example, when applying these coatings, silicone-based finishing processes often produce toxic wastewater, particularly residual treatment fluids, which can be harmful to aquatic life such as fish [25].

Lastly, the scalability and economic viability of non-fluorinated DWR materials remain significant challenges. For example, silicone-based and hydrocarbon-based coatings benefit from mature production processes and relatively low initial costs, whereas hydrocarbon-based coatings have higher long-term maintenance expenses. On the other hand, the complex synthesis process, long production cycle, and high R&D cost of dendrimer coatings further hinder their large-scale application [27]. Addressing these technical, environmental, and economic challenges remains crucial to promoting the practical application and wider market adoption of non-fluorinated DWR materials.

1.5. Scope of article

In this article, the basic concepts, and fundamental relationships pertaining to hydrophobicity, wettability, and stain-resistance are discussed, which include the Cassie-Baxter state, contact angles, and solid surface energy. The non-fluorinated durable water-repellent and stain-resistant coating are deciphered from the basis of knowledge. The role of micro-nano structure in imbuing water repellency is analyzed by examining the surface characterization and the forming mechanism in

DOI: 10.54254/2755-2721/2026.KA29339

natural surfaces such as lotus leaves, shark's skin, exploring the principle of superhydrophobic property in plants and animals. By, comprehensively evaluating the surface morphology for various natural, water repellent surfaces, we aim to create a more comprehensive understanding of the role of surface roughness. Next, to investigate contemporary non-fluorinated DWRs' properties, this article explains superhydrophobicity from a surface energy and roughness perspective. Integrating theory and broad new techniques in the DWR field, this review introduces state-of-the-art methods utilized in the literature to increase surface roughness and decrease the surface energy without the use of fluorinated compounds. In addition, this article summarizes the newest synthesis technologies in the field and the applications of non-fluorinated DWR. In order to examine whether it is feasible to use non-fluorinated DWR to supplant the fluorinated DWR, the review choses two representative materials from four types of non-fluorinated DWR to compare their various properties, such as durability, environmental friendliness, and so on.

2. Theory

2.1. Wettability

Wetting is a key phenomenon in surface and interfacial science, describing how a liquid behaves upon contact with a solid surface. The extent of wetting is largely determined by the balance of surface energies between the solid, liquid, and vapor phases [28]. One of the most widely used parameters to evaluate wetting is the contact angle, defined as the angle between the solid surface and the tangent to the liquid–vapor interface at the three-phase contact line [29]. Young's contact angle (θ_Y), derived from Young's equation, is the contact angle for an ideal solid surface that is atomically smooth, chemically homogeneous and inert, and mechanically nondeformable by the liquid: [30]

$$\cos\theta_Y = \frac{\gamma_{SV} - \gamma_{SL}}{\gamma_{LV}} \tag{1}$$

In Equation (1), γ_{SV} and γ_{SL} represent the interfacial tensions at the solid–vapor and solid–liquid interfaces, respectively, while γ_{LV} denotes the surface tension at the liquid–vapor interface [29]. Surfaces showing contact angles below 90° are classified as hydrophilic, whereas those above 90° are hydrophobic. When the static water contact angle exceeds 150°, the surface is termed superhydrophobic [28].

Different from the ideal surface, real surfaces typically possess multiscale roughness, chemical heterogeneity and/or irreversible adhesion, so the contact angle spans an interval [31]. Its upper limit is the static advancing angle (θ_a) and its lower limit is the static receding angle (θ_r) [4]. As shown in Equation (2), contact angle hysteresis (CAH) is defined as the difference between θ_a and θ_r[32].

$$CAH = \theta_a - \theta_r \tag{2}$$

A lower CAH indicates that droplets detach from the surface more easily, while a higher CAH implies stronger adhesion [25].

Another important descriptor of dynamic wetting is the sliding angle (SA), defined as the lowest inclination required for a droplet to roll off. A reduction in CAH typically results in a lower SA,

DOI: 10.54254/2755-2721/2026.KA29339

facilitating droplet motion [25]. In 1962, Furmidge proposed a predictive model for droplet motion by linking SA to CAH [33]:

$$sin\alpha = \frac{w \times \gamma_{LV}}{mg}\left(cos\theta_r - cos\theta_a\right) \tag{3}$$

where m is the mass of the droplet, g is the acceleration due to gravity, w represents the contact perimeter of the droplet, and α is the sliding angle of the droplet on the solid surface [25]. A lower value of implies stronger liquid repellency, allowing the droplet to roll off more easily [25].

The Wenzel model and the Cassie–Baxter model are generally employed to interpret how surface roughness influences the apparent contact angle (θ^*) of liquid droplets, as illustrated in Figure 1 [34].

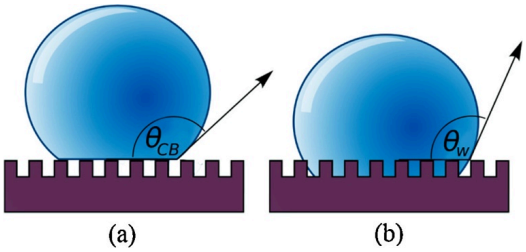

Figure 1. Wetting states of a droplet on a rough surface: (a) Cassie–Baxter state, (b) Wenzel state. Images adapted from prior work [35]

On rough surfaces, a droplet may adopt a fully wetted state in which the liquid penetrates into all surface grooves beneath it, as described by the Wenzel model proposed in 1936 [36]. According to Wenzel's model, the apparent contact angle is given by the following Equation (4) [37]:

$$cos\theta_W = r \times cos\theta_Y \tag{4}$$

where θ_W is the Wenzel apparent contact angle on a rough surface, and r is the surface roughness ratio, calculated as the actual surface area divided by the geometric (projected) area [36]. Wenzel proposed that the contact area between a liquid droplet and a rough solid surface is greater than that on a smooth one [36]. If the solid–liquid interfacial energy is lower than the solid–vapor interfacial energy, wetting the rough surface leads to a more substantial energy decrease, thereby enhancing the wetting process [36]. In contrast, when the solid–liquid interfacial energy is higher, the surface exhibits an intrinsic resistance to wetting, making it considerably harder for the liquid to spread across the rough surface [36]. This implies that surface roughness amplifies the inherent wetting characteristics of a material. Specifically, when a smooth surface is hydrophilic, increasing its roughness enhances its hydrophilicity. Conversely, if the surface is inherently hydrophobic, roughness further strengthens its water-repellent behavior [36].

Another possible wetting state for a droplet on a rough surface is the Cassie–Baxter mode, in which the droplet is supported by the tops of surface protrusions while air is trapped in the cavities beneath, forming a composite solid–air–liquid interface [36]. Cassie and Baxter originally formulated the following Equation (5) to characterize this wetting state [38]:

DOI: 10.54254/2755-2721/2026.KA29339

$$cos\theta_{CB} = f_{SL}cos\theta_1 + f_{LG}cos\theta_2 \tag{5}$$

where θ_1 and θ_2 correspond to the contact angles of the liquid on the solid surface and on the trapped air, respectively [34]. The parameters f_{SL} and f_{LG} represent the area fractions of the droplet in contact with the solid and the air within the surface cavities, with $f_{SL} + f_{LG} = 1$[34]. Within this composite interface, the solid region is considered completely wetting ($\theta_1 = 0^\circ$), while the air region is entirely non-wetting ($\theta_2 = 180^\circ$) [34]. Based on these conditions, the Cassie–Baxter equation simplifies to [38]:

$$cos\theta_{CB} = f_{SL} \times (cos\theta_Y + 1) - 1 \tag{6}$$

Under this model, the intrinsic wetting properties of the surface are also further intensified.

2.2. Water-repellency

Certain materials possess a natural property of water-repellency, which makes it difficult for water falling on their surface to stick to them but rather easy to roll off and bounce back from their surface, regardless of whether the material is natural or synthetic [39].

2.2.1. Surface tension of liquid

In a state of static equilibrium, the surface of a liquid—upon which a small-mass object, such as a needle, is placed—demonstrates characteristics akin to those of a stretched elastic film. Despite the fact that the needle is composed of metal and therefore possesses a density significantly greater than that of most liquids, and notwithstanding the expectation based on Archimedes' principle that it should sink, the needle remains suspended on the liquid surface. This phenomenon arises due to the surface tension of the liquid, which generates a supporting force sufficient to counterbalance the weight of the metal needle.

Intermolecular force could be used as the elementary explanation of the surface tension. Molecular theory of liquids suggests the molecules of the intermolecular attraction force is effective over a distance of around ten times of molecular diameter. The distance from the molecular center is the determinant of the magnitude of such attractive force. In approximation, the critical value of the distance for the intermolecular attraction to be zero is 10-7 cm from the center of a small molecule that is neither stationary nor spherical. A molecule in liquids or at a distance within 10-7 cm has a zero resultant force since it is completely surrounded by other molecules, while a molecule at the surface of liquids is impacted by a downward resultant force as the upward attactive force of the gas molecules above is much smaller than the downward attactive force of the liquid molecules. This downward resultant force of the molecule acts on the surface and gives rise to it, which is also a potential energy, is known as surface tension.

According to principle of lowest energy, all the systems have a common tendency of keeping a minimum potential energy. Hence, liquids are expected to exist in a shape with the smallest surface area, and the force per unit length that opposes the expansion of the surface area is the surface tension of a liquid [40]. With constant volume, composition, and temperature, the surface tension of liquid could be expressed as:

DOI: 10.54254/2755-2721/2026.KA29339

$$\gamma = \left(\frac{\partial A}{\partial \mathscr{A}} \right)_{N,V,T} \tag{7}$$

where A is the Helmholtz free energy and $\mathscr{A}$ is the surface area. The corresponding expression includes the Gibbs free energy G is [41]

$$\gamma = \left(\frac{\partial G}{\partial \mathscr{A}} \right)_{N,P,T} \tag{8}$$

When a droplet on a surface is composed of a pure liquid, the surface of liquid (γ_L) is equal to the liquid-gas interfacial force per unit length of the contact line (γ_{LV}) [42].

2.2.2. Surface energy of liquid

A new solid surface can be regarded as a result of a reversible thermodynamic process. Under inert conditions or in a vacuum, the amount of work required to create such a surface-regardless of the specific method used-is referred to as the solid surface energy (γ_S). The surface energy of solids corresponds to the partial free energy of the solid associated with the reversible reorganization of solid's electron structure near the surface.

In general, the surface energy of solids is treated as the sum of components arising from polar interactions such as hydrogen bonding (γ_{SD}) and non-polar interactions such as dispersion force (γ_{SP}):

$$\gamma_S = \gamma_{SD} + \gamma_{SP} \tag{9}$$

2.2.3. Solid-liquid interfacial energy

The surface tension related to solid cannot be measured directly, but the strength of adhesion to a solid surface can be derived from the thermodynamic concept of the "work of adhesion (W_a)" in a three-phase system:

$$W_a = \gamma_S + \gamma_L - \gamma_{SL} \tag{10}$$

and

$$W_a = \gamma_L(1 + cos\theta) \tag{11}$$

where θ is the contact angle between the solid-liquid interface, γ_S , γ_L , and γ_{SL} are the tension of the solid-air, the liquid-air interface, and the solid-liquid interface respectively. By rearranging these two equations, the solid-liquid interfacial energy can be expressed in the form [43]:

DOI: 10.54254/2755-2721/2026.KA29339

$$\gamma_{SL} = \gamma_S - \gamma_L cos\theta \tag{12}$$

2.2.4. Contact angle

A surface is considered hydrophobic when the contact angle exceeds 90 degrees, and superhydrophobic when the contact angle exceeds 150 degrees. For obtaining higher the water repellency i.e. water contact angles, we need a low surface energy for the solid, and a large solid-liquid interfacial tension [44].

2.2.5. Wettability spreading coefficient

When two interfaces—such as a liquid-(a)/gas interface and a liquid-(a)/liquid-(b) interface—approach each other within a pore, the fluids will spontaneously redistribute at a certain point. In this situation, if liquid-(a) spreads over liquid-(b) in the presence of gas, the wettability spreading coefficient is the most appropriate parameter to describe this condition. It is defined as:

$$S_{a/b} = \delta_{a/g'} - \delta_{b/g'} - \delta_{a/b'} \tag{13}$$

Here, $S_{a/b}$ is the final wettability spreading coefficient, while $\delta_{a/g'}$, $\delta_{b/g'}$ and $\delta_{a/b'}$ are the respective interfacial tensions under conditions where the three fluids are in thermodynamic equilibrium. When a unit area of liquid-(a) is covered by a thick flat film of liquid-(b), the real-time wettability spreading coefficient actually describes a non-equilibrium situation.

The numerical value of the final wettability spreading coefficient derived from the equation above can be either positive or negative. Generally, when $S_{a/b} > 0$, liquid-(a) will spread over liquid-(b); when $S_{a/b} < 0$, liquid-(a) will not spread over liquid-(b) since it is energetically unfavorable for liquid-(b) to be covered by liquid-(a).

The definition of wettability spreading coefficient is also applicable for three-phase systems (gas-liquid-solid). In such cases, the larger the numerical value of the coefficient S, the stronger the water-repellency.

2.3. Stain-resistant

In general, stain-resistant refer to the ability of fabrics to withstand and avoid the perpetual adhesion of stain agents such as liquid, dust and mud [45]. In addition to the numerous common methods to increase the hydrophobicity and breakthrough pressure, researchers have developed alternative scenarios to repel the viscous liquid or evade dust and other stains.

Another path can be the photocatalytic activity. It is a process catalyzed by light which promotes the redox reaction with substance in environment. Through photocatalytic activity, coating can produce free radical to react with the stain [46].

A typical instance should be the TiO_2NPs(nanoparticles)-coated cotton fabric: when light is equal or greater than the band gap energy, the electron will absorb the energy and get rid of shackle from the atomic nucleus. During this process, TiO_2 will produce the valence-band holes (h^+) and conductive-band electron (e^-) [47].

DOI: 10.54254/2755-2721/2026.KA29339

$$TiO_2 + hv \rightarrow h^+ + e^- \tag{14}$$

Secondly, the produced h+ and e- will facilitate the redox reaction with the surrounding element. For example, holes can react with hydroxyl group in water to form the hydroxyl radical (•OH) and electron can react with O2 to form superoxide radical anions O_2• and •HO_2 [48].

$$h^+ + H_2O \rightarrow \bullet OH + H^+ \tag{15}$$

$$e^- + O_2 \rightarrow \bullet O_2^- \tag{16}$$

Next, these radicals which are highly reactive can react with the organic compound which means the stain adhere on surface can be cancelled and transformed into inoffensive molecules such as CO_2 and H_2O when they meet the radicals.

$$\bullet OH + R - CH_3 \rightarrow R - CH_2 \bullet + H_2O \tag{17}$$

2.4. Hydrophobicity of fluorinated materials

Fluorinated materials, especially those containing perfluorinated alkyl chains, achieve outstanding water and oil resistance because of their distinct molecular structure and surface characteristics. The key to this performance lies in the carbon-fluorine (C-F) bond. This bond has high energy and low reactivity. Importantly, fluorine is the most electronegative element and has a small atomic size. Together, these factors produce a dense, symmetrical electron cloud around the C-F bond [49]. This cloud greatly reduces interactions between the surface and contacting liquids. As a result, fluorinated compounds, particularly those with linear perfluorinated sections (e.g., -CF_2-CF_3), show an extremely low critical surface tension (often below 20 millinewtons per meter or mN/m) – a value significantly lower than what hydrocarbon-based materials can achieve.

Moreover, unlike bonds such as carbon-hydrogen (C-H), the tightly held electrons in C-F create surfaces that strongly repel both water and oils. Water exhibits high surface tension (approximately 72 mN/m), while oils typically have lower values (around 20-35 mN/m). When these liquids contact a fluorinated surface—which possesses an ultra-low critical surface tension—they form high contact angles as described by Young's equation [30]. Essentially, fluorinated materials drastically reduce the solid's surface tension (γ_{SV}), resulting in contact angles typically well above 90° (often exceeding 100°) for water, and remarkably, also above 90° for many oils. This causes droplets to bead up and roll off easily, demonstrating outstanding resistance to both water- and oil-based substances.

Additionally, the straight and rigid structure of perfluorinated chains allows them to pack tightly and stand upright at the surface. This arrangement maximizes the presence of terminal -CF_3 groups, which have the lowest possible surface energy, creating a smooth, dense outer layer with minimal surface energy. This natural resistance to water and oils, combined with the ability to design surface textures, enhances the coatings' effectiveness. Even on microscopically rough surfaces (known as the Wenzel state), their inherently low surface energy preserves repellency. More importantly, they

DOI: 10.54254/2755-2721/2026.KA29339

easily form stable Cassie-Baxter interfaces where air pockets are trapped under liquid droplets [50]. This drastically reduces contact between the solid and liquid, lowering adhesion forces and enabling droplets to roll off easily (self-cleaning). Long-chain perfluoroalkyl (e.g., C_8F_{17}) compounds exhibit superior crystallinity, enabling tighter molecular packing and lower surface energy. This results in enhanced water repellency and long-term durability. In contrast, short-chain variants (e.g., C_6F_{13}, C_8F_9) possess poorer crystallinity [24]. Long-chain perfluoroalkyl compounds demonstrate enhanced crystalline ordering and denser molecular packing, facilitating the formation of a thermodynamically stable low-surface-energy layer. This structural configuration consequently confers superior water and oil repellency alongside augmented durability. Conversely, short-chain variants exhibit compromised crystallinity and disordered molecular alignment, yielding both elevated surface energy and reduced interfacial stability. These inherent limitations significantly diminish repellent efficacy and compromise functional longevity. Together, these effects significantly boost the longer chain coating's water/oil resistance and stain protection.

In summary, fluorinated materials achieve water resistance through two key mechanisms: molecular-level properties (the low surface energy of C-F bonds) and surface-level design (surface roughness interaction). This dual approach explains their long-standing dominance in waterproofing.

3. Natural water repellent surfaces

3.1. Lotus leaf

The lotus leaf is the canonical natural template for superhydrophobicity, characterized by extremely high contact angles and very low roll-off angles. This remarkable water-repellent and self-cleaning property is commonly referred to as the "lotus effect" [51]. Its extreme repellency originates from a distinctive micro–nano papillary architecture and a low-surface-energy non-fluorinated wax layer [49]. Scanning electron microscopy shows that the leaf's top surface consists of conical papillae approximately 5-15 μm in diameter and 10-20 μm in height, constituting the principal layer of surface roughness, as shown in Figure 2 [53]. Superimposed on these papillae are nanoscopic wax crystals with typical feature sizes of 100-200 nm that establish the secondary textural tier [53]. The surface wax is primarily composed of C29-C33 alkanes, whose outward-facing methyl termini depress the surface free energy to about 25 mN m^{-1} [53].

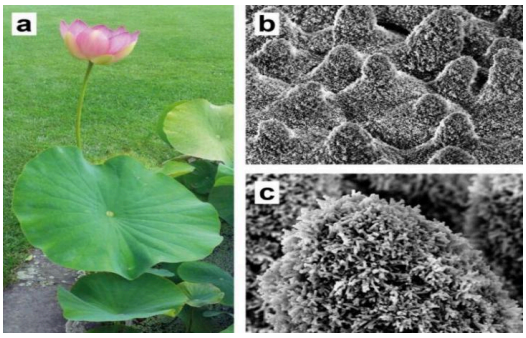

Figure 2. a) Photograph of a lotus plant. b) Scanning electron microscopy micrograph of the lotus-leaf surface showing a hierarchical architecture; the primary tier comprises micrometre-scale conical papillae derived from epidermal cells. c) These papillae are cloaked by epicuticular wax crystals, which confer extreme superhydrophobicity. Images adapted from prior work [52]

From a mechanistic perspective, the exceptional wettability of the lotus leaf is well described by the Cassie–Baxter model [53]. In this framework, water droplets are supported by the tips of the

DOI: 10.54254/2755-2721/2026.KA29339

surface papillae, with air pockets retained in the interstitial spaces below. Such a configuration greatly reduces the fraction of the liquid in contact with the solid substrate, thereby elevating the apparent contact angle to values as high as 162°, which is firmly within the superhydrophobic range [53]. Moreover, the presence of these underlying air cushions also yields remarkably low roll-off angles, frequently below 5°, allowing droplets to detach and roll away with minimal inclination, effectively removing surface contaminants [53]. This natural design has become an archetype for the engineering of synthetic surfaces and coatings that seek to emulate the lotus leaf's outstanding wetting resistance.

3.2. Shark's skin

Shark skin possesses a unique microstructure defined by numerous overlapping, tooth-like scales known as dermal denticles. These denticles, which constitute the skin's primary structural element, are arranged in a highly ordered pattern rather than randomly distributed. Each denticle features a complex morphology, typically comprising a raised crown anchored by a base embedded within the dermis. While denticle size, shape, and spacing exhibit interspecies variation, they universally generate a riblet-like surface topography. These riblets typically feature a triangular or rounded cross-section, with heights ranging from 50 to 200 micrometers and spacing between adjacent riblets measuring approximately 100 to 300 micrometers, forming a periodic microscale undulation across the skin surface (Fig. 3) [54]. Notably, fast-swimming species such as the mako shark exhibit more pronounced and regular riblet structures, an adaptation thought to optimise hydrodynamic drag reduction.

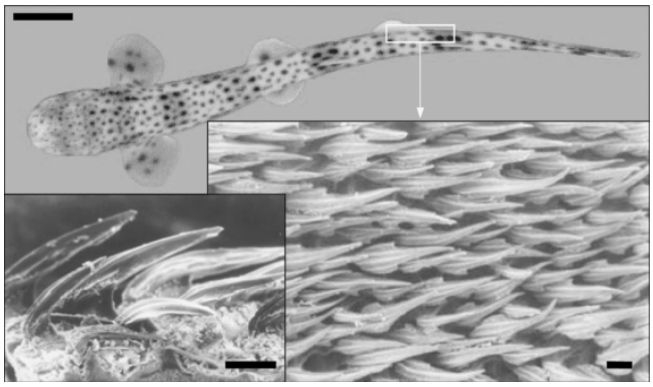

Figure 3. Morphology of dermal denticles in the lateral caudal region of a juvenile dogfish (white rectangle). The scale bar is 10 mm. First inset, surface view of the denticles; second inset, transverse view of the denticles illustrating their extension above the skin surface. Scale bars, 200 µm. Images adapted from prior work [54]

From a wettability perspective, the denticle-induced micro-roughness critically governs the skin's interaction with water. This surface architecture can be interpreted through modified Wenzel and Cassie-Baxter wetting models. Specifically, as the shark moves through water, the denticles likely facilitate a composite solid-air-liquid interface, analogous to the Cassie-Baxter state, by entrapping air or vapour pockets. Consequently, this minimises the actual contact area between the skin and water, significantly reducing molecular adhesion [55]. The resultant hydrophobic tendencies contribute not only to drag reduction but also appear to inhibit marine biofouling, although the precise anti-fouling mechanism—potentially involving synergistic physical and chemical factors—remains under investigation.

DOI: 10.54254/2755-2721/2026.KA29339

3.3. Insects' ommateum

Surfaces are prone to misting when droplets with diameters exceeding half of the shortest wavelength of visible light—around 190 nm—condense and coalesce on them. This phenomenon presents a considerable challenge to the visual capabilities of insects, as they lack eyelids. In contrast, the presence of such a structure in other organisms can significantly reduce the accumulation of moisture and contaminants, thereby effectively mitigating external factors that impair vision [56].

Among all insect species belonging to the family Culicidae, the mosquito is notable for its extraordinary vision, which remains effective even in dim light and humid air, enabling it to locate mates, suitable sites for oviposition, and sources of food (blood). The surface of each unit of the compound eye—an insect's optical sensory unit known as an ommatidium—is covered with numerous nanoscale nipple-like protrusions. With diameters of roughly 100 nm and spacings of approximately 50 nm, these hexagonal, non-close-packed structures (see Figure 4) create an air gap that minimizes the contact area between water and the surface, while also producing a composite, non-planar, energetically less favorable, three-phase wetting interface.

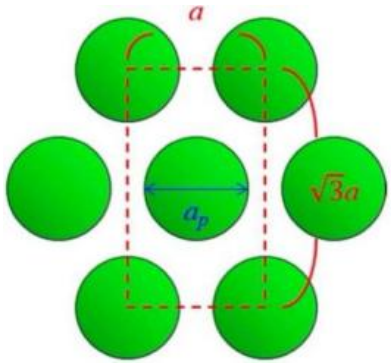

Figure 4. Non-close-packed hexagonal arrangements of subwavelength structure. Images adapted from prior work [57]

Beyond mosquitoes, other insects also possess similar water-resistant eye-surface structures composed of patterned, bubble-like bulges with diameters within 100 nm and small separation distances. Species such as Lucilia sericata (the green bottle fly), moths, and many others exhibit this adaptation, which reduces interfacial hydrogen bonding at the water–solid interface on nanostructured surfaces. Night-flying moths, in particular, aquire a layer of a subwavelength structures that covers their eyes (see Figure 5) [57]. Though the principal function of subwavelength structures is to eliminate reflection of visible light, Wen-Kai Kuo and his team found that a non-close-packed polystyrene (PS) nanosphere monolayer, which replicates such a structure on the surface of glass substrate, also exhibits water-repellent properties.

The surface roughness of NOA 63-coated glass can be significantly enhanced by treating the PS nanosphere monolayer with oxygen plasma. The duration of plasma treatment serves as the primary factor determining the resulting contact angle of the AR specimens. Four sets of samples were treated for different lengths of time: 0 min, 2.5 min, 5 min, and 10 min, resulting in contact angles of 109.7°, 119.7°, 98.4°, and 86.9°, respectively. The hydrophobicity exhibited by these AR specimens, which incorporated parabola-shaped subwavelength-structured NOA 63 coatings, was attributed to the increased surface roughness. This finding suggests that such plasma surface treatment offers a promising alternative to conventional fluorinated DWRs, which pose environmental and health risks.

DOI: 10.54254/2755-2721/2026.KA29339

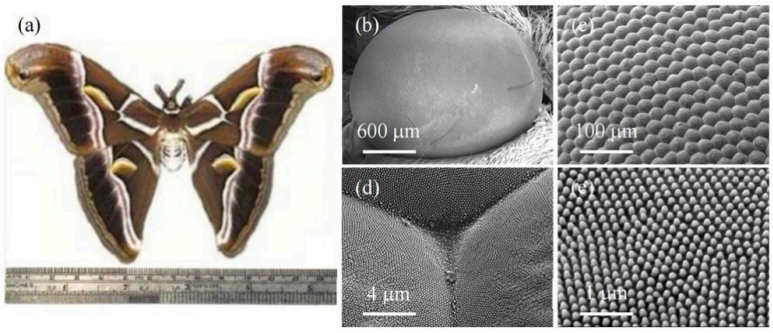

Figure 5. (a) The photograph of an adult Philosamia cynthia ricini obtained from the Miaoli District Agricultural Research and Extension Station, Council of Agricultural, Taiwan; SEM images of the Philosamia cynthia ricini moth-eye structure at different magnifications: (b) the complete compound eyes, (c) the hexagonal arrangement of ommatidia, (d) the details of the ommatidia, and (e) the corneal nipple arrays in one ommatidium. Images adapted from prior work [57]

3.4. Spider silk

Spider silk is a natural polypeptide, polymeric protein, and is in the scleroprotein group. In general, spider silk consists of approximately 42% glycine and 25% alanine as the major amino acids, along with other relatively larger amino acids, such as glutamine, serine, leucine, valine, and proline, whose components depend on factors including diet and species [58]. From a micro-perspective, according to the Figure. 6, alanine forms an ordered region called “crystallized region” and glycine forms “amorphous region” which are both connected by peptide linkage through dehydration synthesis reaction. With a -CH3 side chain and a small volume, the alanine protein can easily form β-sheet nanocrystals, which are stabilized by inter-strand hydrogen bonds between backbone N–H and C=O groups. The β-sheet region acts as a rigid domain, preventing large-scale slippage and contributing to silk's high stiffness and strength. In addition, as the smallest amino acid, glycine possesses an extremely small steric strand so that it can readily form various conformations, such as β-turn, and result in a disordered region. This region bestows spider silk a flexible property, given that the silk can stretch and absorb energy without breaking even if it is placed in a high temperature [59].

In the organ that produces spider silk, the spidroin is soluble because the environment inside the silk gland is basic. As a result, some terminals such as carboxyl terminus will have charges, which makes the substances form “ion-dipole interaction” with water and bury the hydrophobic chain so that these monomers won’t approach each other. When spidroin goes through the spinning duct, the pH will decrease throughout the duct. Accompanied by the acidic environment, some hydrophilic groups will be protonized ($COO^- + H^+ \rightarrow COOH$) [60].

During this process, a phenomenon called salt bridge, which means the remaining ions with different charges will attract each other and lock two N-terminal domains, forming a dimer. The dimer facilitates the whole protein to be parallel with and aligned with others. Because of the salt bridge, the hydrophobic groups can appear in the solution. It promotes molecules to self-assembly because the hydrophobic group can help molecules cluster together to form a β-sheet nanocrystal. Under the sheer force of the narrow duct, the silk will be shaped in a straight line and finally constitute a web [61].

DOI: 10.54254/2755-2721/2026.KA29339

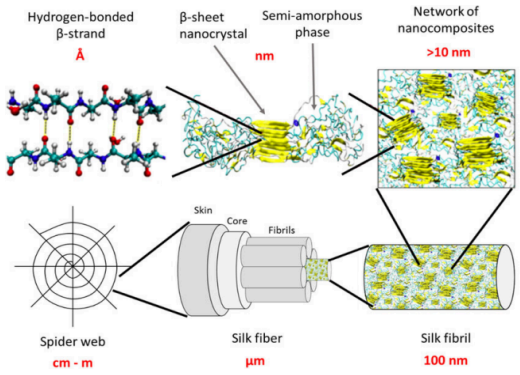

Figure 6. The hierarchical structure of spider silk, from hydrogen-bonded chains to macroscopic web structures, covering multiple length scales. Images adapted from prior work [62]

The reasons why spider silk can have such a remarkable superhydrophobic property are the hierarchical structure and nonpolar molecules constituting the silk. The β-sheet nanocrystal is so dense that water molecules can't penetrate into the layers. Amino acids like alanine, leucine, and valine are nonpolar side chains, which can't form a strong interaction with water, causing them to be hydrophobic. Moreover, the nano-micron structure in silk makes it possess a high roughness. The network of nanocomposites offers a complex surface as shown in the figure 7, the hierarchical structure allows air to flow in the surface so that increase the contact angle between water and the silk. By Integrating low surface energy and high roughness, spider silk shows an excellent superhydrophobic property by using only non-fluorinated materials [63].

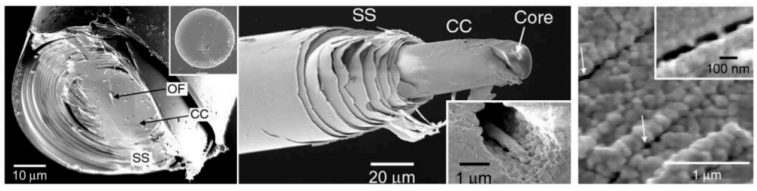

Figure 7. Structural characterization of the basalia spicules. Images adapted from prior work [64]

4. Non-fluorinated coating materials

4.1. Spider silk

4.1.1. Surface energy

Surface energy constitutes a fundamental thermodynamic property dictating the interfacial interactions between a solid material and its surrounding medium, particularly aqueous or oleophilic phases [65]. This intrinsic property arises from the excess energy inherent at the material's surface, resulting from asymmetric intermolecular forces: cohesive interactions equilibrate within the bulk phase, whereas surface molecules experience uncompensated forces, generating residual energy [66]. Consequently, surface energy directly governs wettability phenomena—manifested as the propensity of a liquid to spread or form discrete droplets—rendering its precise characterization indispensable for the development of non-fluorinated durable water repellent coatings.

The fundamental principle underpinning water repellency resides in minimizing the coating's surface energy relative to that of the target liquid. Given water's characteristically high surface tension (approximately 72.8 mN/m at 20°C), materials exhibiting depressed surface energies

DOI: 10.54254/2755-2721/2026.KA29339

inherently resist aqueous wetting. The equilibrium contacts angle (θ), established at the solid-liquid-vapour interface, is quantitatively described by Young's equation: $\cos\theta = (\gamma_{sv} - \gamma_{sl})/\gamma_{lv}$, and γ_{sv} denote solid-vapour surface energy, γ_{sl} is solid-liquid interfacial energy, and γ_{lv} is liquid-vapour surface tension, respectively. Critically, a reduction in γ_{sv} promotes an increased contact angle, thereby inducing droplet bead formation and subsequent roll-off rather than surface wetting [29].

Conventional fluorinated coatings achieve exceptional hydrophobicity through ultralow surface energies (typically <20 mN/m), a trait rooted in the strong electronegativity and stability of carbon-fluorine (C-F) bonds that minimize surface intermolecular interactions. For non-fluorinated alternatives, the primary challenge is replicating this low-energy state using sustainable chemistries. Key strategies focus on integrating molecular components that naturally reduce surface polarity: hydrocarbon systems with long alkyl chains (e.g., C18–C24 derivatives) create nonpolar surfaces with energies around 25–30 mN/m [67]; silicone-based formulations, particularly polydimethylsiloxanes (PDMS), leverage methyl-terminated backbones to reach 20–24 mN/m, closer to fluorinated levels [68]; and bio-derived materials like plant waxes offer renewable options with energies of 28–35 mN/m [69]. While these approaches confer meaningful water repellency, bridging the performance gap with fluorinated materials demands further optimization—such as enhancing molecular packing or combining chemical design with surface structuring to balance low energy with durability.

In the development of non-fluorinated durable water repellent coatings, surface energy optimization must be synergistically balanced with durability enhancement. While reducing surface energy augments hydrophobicity, it may concurrently compromise mechanical robustness or interfacial adhesion to substrates. Consequently, meticulous molecular engineering of surface energy emerges as a critical design strategy. This approach ensures the resultant coating achieves both effective water repellency and long-term structural stability under operational stressors. A comprehensive understanding of surface energy is therefore fundamental to engineering high-performance non-fluorinated coatings capable of meeting stringent application requirements.

4.1.2. Roughness

As another imperative trait of a superhydrophobic surface, roughness plays an essential role in whether the surface can repel water and increase its contact angle. Increasing surface roughness, typically increases the water-air interfacial area, yielding higher contact angles / increased water repellency. Several methods have been previously utilized to increase surface roughness.

4.1.2.1. Fluorine-free nanoparticle coating

Sol-gel-derived silica nanoparticle (NP) and silica-ZnO NP have been widely used to fabricate water-repellent surfaces. Shown in Figure 8, at first, the TEOS($Si(OC_2H_5)_4$) reacts with hydroxide under basic conditions via ammonia-catalysed hydrolysis to form a silanol, which condenses to the siloxide ions and water. By attacking the silanol silicon centre, the siloxane linkage network forms on the surface of the NP. In the process, siloxane will form a Si-O-Si bond at the center. Secondly, through double-jet precipitation, ZnO addition can be completed in several steps: Zn^{2+} will initially form the β-$Zn(OH)_2$, which rapidly transforms into ZnO. Under ethanolic conditions, the smaller, well-dispersed NP sizes will be formed. $Zn(OAc)_2$ is decomposed into interstices of inorganic silica network, resulting in Si–O–Zn and Si–O–Si bands, corresponding to a strong bonding interaction between ZnO and the silylating agent. In addition, triethylamine (TEA) can activate the siloxane silicon and facilitate the reaction between Zn^{2+} and silicone to form ZnO molecular clusters that can

DOI: 10.54254/2755-2721/2026.KA29339

readily attach to the silica surface. After the addition of ZnO, PDMS will hydrolyze first to form a polymer and then cross-link together, which mixes with the NP and attaches to the coating [70].

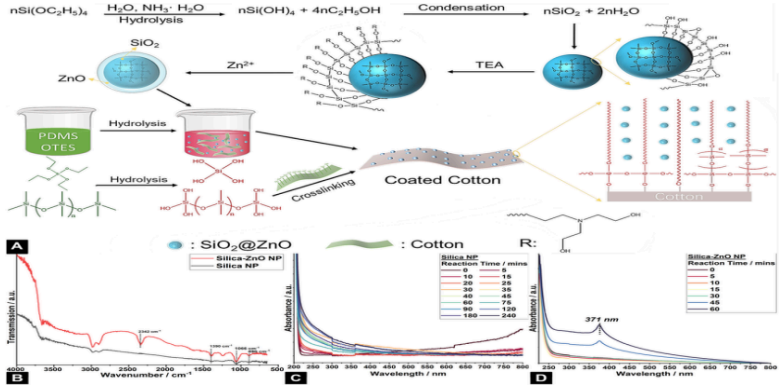

Figure 8. The procedures of creating a nanoparticle coating. Images adapted from prior work [71]

From the superhydrophobic perspective, the silica nanoparticle illustrates a clear presence of discontinuous spikes and clusters. Because of the nanoparticle clusters, the roughness of the whole surface increases, allowing air to go through between clusters. As a mature technology, NP indicates good durability of the coating. Even if washed or exposed under UV light, the nanoparticle can still persistently adhere to the surface. The surface it offers enlarges the effect of the energy siloxane provides and helps water stay on the complexed surface [72].

4.1.2.2. Plasma-based treatment

Plasma-based treatment refers to the technology that utilizes electrodes or other magnetic elements to ionize the fluid around the electrically charged conductor. Either plasma or neutral molecules (atoms and radicals) can etch the surface to shape it with micro- and nano-scale structures. As an environmentally friendly technology with relatively low cost, plasma-based treatment is widely used to empower the textile's hydrophobic property [73].

In general, the plasma used in technology is cold by applying the electrical field over two electrodes with a gas in between, which means the electrons will acquire a higher energy than other molecules or atoms. Given that electrons only make up over 1/1,000,000 of the total mass, the temperature of the holistic plasma mixture is cold. The plasma treatment can be divided into two categories: atmospheric plasma treatment and low-pressure plasma. In particular, atmospheric plasma involves atmospheric pressure plasma jet (APPJ) and dielectric plasma treatment (DBD) [74]. According to Figure 9, firstly, electrons can be activated by applying a high voltage or radio-frequency (RF). Then, electrons at a high speed collide with the gas molecules such as nitrogen, oxygen, and helium, which generate reactions like ionization, activation, and dissociation (the reaction forms free radicals). Following the reaction, the formed molecules collide with other gas molecules and form more radicals, molecules in excited states, and ions. These particles react with the textile and etch the surfaces by breaking the bonds of fabrics and oxidizing the organics over the surfaces. Moreover, particles are able to fragment the precursor [75]. For instance, hexamethyldisiloxane (HMDSO) has been shown to it can be fragmented by the energetic particles, and forms Si• and CH_3• radicals. These radicals can form a Si-O-Si network over the surfaces with a CH_3 side chain, ensuring a low surface energy for better superhydrophobic property. However, it is easy to form an electric arc between two electrodes during the process. As a result, the dielectric barrier is added in one of the electrodes to prevent electricity from being produced (DBD). Low-

DOI: 10.54254/2755-2721/2026.KA29339

pressure plasma, by contrast, must be held in the vacuum chamber after evacuating all gas from the container. Next, the process gas enters the container and embarks on being ionized. This type of plasma can etch the surface uniformly without any concerns of health and environmental issues or surface ablation. The surface produced by the plasma offers a clear micro-nano structure, which indicates it can increase the roughness continuously and stably [76].

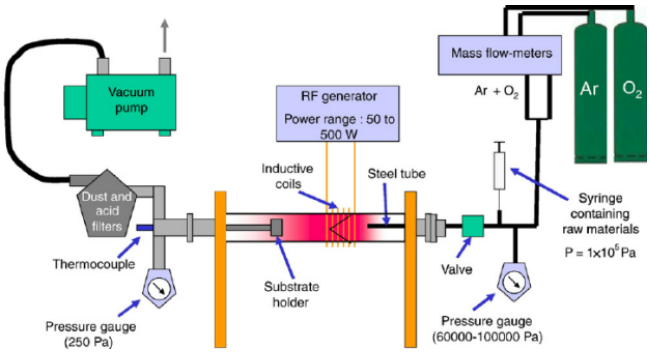

Figure 9. The brief description of the low pressure plasma equipment. Images adapted from prior work [77]

4.1.2.3. One-bath spraying process / photothermal self-healing performance

Playing as a broad new type of technology, increasing the roughness, the one-bath spraying process introduces a powerful and cheap way to manufacture the superhydrophobic surfaces in the future. Rather than etching textile surfaces to create the roughness, the one-bath spraying process utilizes a solution to "add" a rough layer over surfaces.

One-bath spraying process, in fact, is composed of two procedures. Bathing means fabrics are immersed in the solution, which includes polymers, nanoparticles, and so on. The molecules dissolved in the solution can react with the surface of the fabric and cover the fabric with a high roughness layer, which can produce a high contact angle. For instance, in correspond with the Figure 10 Mxene, a solution produced by exfoliating and dissolving the nanoparticle Ti_3AlC_2, is integrated with another polymer solution, polyacrylate (PA), to forge a surface with excellent ultrahydrophobic properties. At first, the surface dips into the Mxene solution and is dried after that procedure. Then, the fabric dips into the PA solution again, followed by another drying. The product not only illustrates superhydrophobic properties but also a photothermal self-healing performance in the experiment. Photothermal self-healing property represents the ability to recover the hydrophobic property after a thermal activity such as UV-radiation. When fabric is washed or destroyed by other daily moisture campaigns, the nonpolar side chains over the surface coil, diminishing the hydrophobic nature. As a result, the polar group, such as -OH, is exposed and favors the ultrahydrophilic behavior. However, after being illuminated by the sun for 20 minutes, the damaged cotton fabric instantly recovers its repellent properties against water. It is because the thermodynamic force drives the nonpolar side chain to extend and uprightly arrange during the radiation [78].

DOI: 10.54254/2755-2721/2026.KA29339

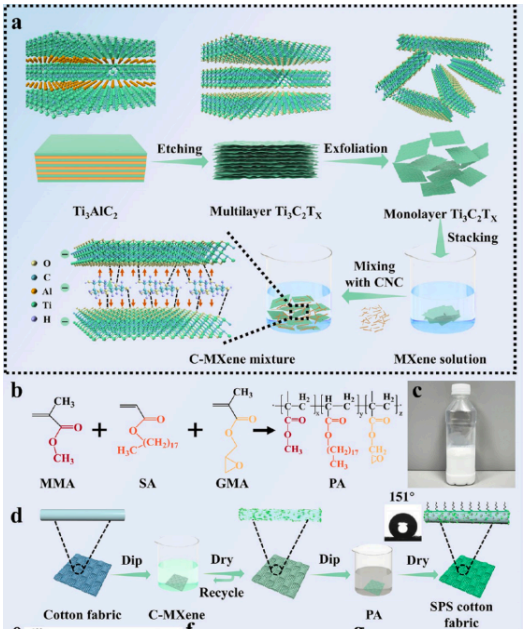

Figure 10. The procedures of creating SPS cotton fabric. Images adapted from prior work [78]

Spraying, by contrast, means the solution is sprayed onto the surface. The solution can include a modifier, curing agent, and epoxy resin, Zeolitic Imidazolate Frameworks (ZIF), a type of metal-organic framework (MOF). These substances endow the surface with a micro-nano structure (shown in the Figure 11)when they are sprayed on the textiles and form a special morphology. After immersing the coating in water, the superhydrophobic coating has a layer of air film on its surface due to its special micro and nano structure, which shows the “silver mirror effect”. In addition, the fabric shows an obvious antifouling effect in the following test, like immersing in methylene blue, given that there is no contamination on the surface [79].

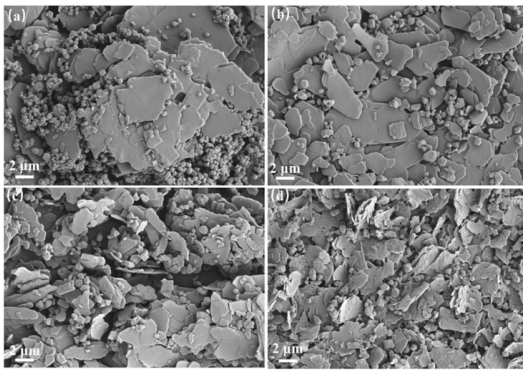

Figure 11. The SEM image of the fabric in 1:2 ratio between ZIFs and different modifiers. Images adapted from prior work [79]

4.2. Synthetic techniques

4.2.1. Sol-gel and siloxane-based coatings

The sol-gel method (shown in Figure 12) is widely used in the industrial preparation of wet chemical materials. When using this technique, the precursor is hydrolysed in the liquid phase. The condensation polymerization of the colloidal particles, on the other hand, provides the gel system.

DOI: 10.54254/2755-2721/2026.KA29339

The surface of the substrate collects the nanoparticles in the system via physical deposition. Although there are many choices of the nanoparticle's fillers, such as SiO_2, TiO_2, Al_2O_3, and SnO_2, SiO_2 is the most commonly used. High chemically active reactants and the correspondent precursors to the nanoparticle fillers tend to polymerize in solution as they are completely mixed together. The nanoparticles then form a cross-linked lattice structure while the gels solidify. Finally, a superhydrophobic coating is formed as the nanoparticle fillers in the solution are captured by the material surface after drying, sintering, and curing. Further enhancements can be made to the coated film, and the superhydrophobicity and other properties of the film can be tailored to specific needs. The gel undergoes dehydropolymerization at a certain temperature to form dense coatings [80].

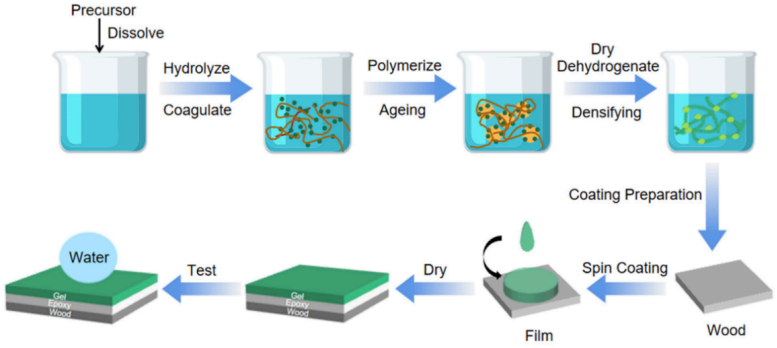

Figure 12. Preparation of superhydrophobic coatings by the sol-gel method. Images adapted from prior work [80]

Different conditions will result in various coating structures depending on the substrate impregnation method. For example, acid catalytic conditions lead to thin silica films, while alkaline catalytic conditions result in loose films composed of spherical silica particles [80]. Besides, the hydrophobicity of the coating increases with the concentration of citric acid in the sol-gel solution [81].

4.2.2. Aerosol-Assisted Chemical Vapor Deposition (AACVD)

Chemical vapor deposition (CVD) is a bottom-up method aimed at forming a thin solid film on a substrate from various gas-phase precursors that have high solubility, low vapor pressure, and low viscosity. Aerosol-assisted chemical vapor deposition (AACVD) is a variation of CVD. In this method, the precursor mixture, dissolved in solvents, is aerosolized by a nebulizer or ultrasonic humidifier and then transported by a carrier gas to the heat reactor under atmospheric or low pressure. A solid film forms in the reactor as the solvents evaporate, while the precursors react either homogeneously or heterogeneously as Fig. 13 demonstrated. Unlike traditional CVD, particles in the precursor mixture diffuse by Brownian motion and eventually reach the cooler glass top plate (substrate) from the heated carbon block. This process, referred to as thermophoresis, includes physisorption. Additionally, AACVD is suitable for depositing oxide and sulfide products, making it feasible for industrial manufacturing of coatings with rough textures. This process depends on the solubility of the precursor [82].

DOI: 10.54254/2755-2721/2026.KA29339

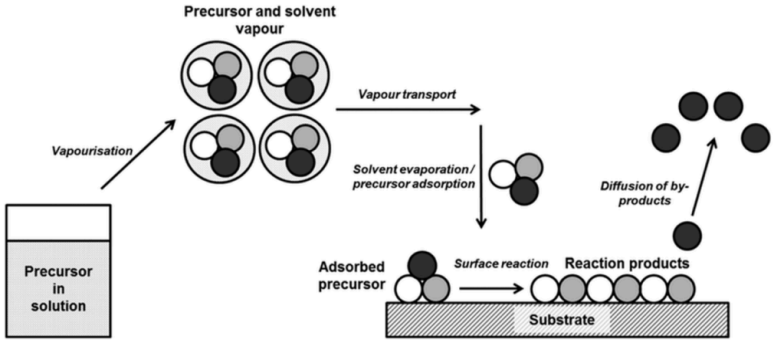

Figure 13. (a) Schematic illustration of AACVD method. Images adapted from prior work [83]

4.2.3. Polymer-nanoparticle composite sprays

The spraying method in the wet chemical process is high-profile for its large scale of production, small limitation on the equipment, and no restriction of the size and the shape of the substrate. The combination of low surface energy adhesives and functional coating is one of the solutions to the environmental issue of the traditional water repellent agent and the non-apparent bonding effect of the non-polar adhesives. In the research conducted by Xu's team, the 5 wt. % of SiO2 hydrophobic dispersion is srayed on the layer of 9 wt. % SBS and C9 petroleum resin (SBS/C9) ethyl solution with substrate made of glass (shown in Fig. 14). The SBS/C9-SiO2 coating tested is corrosion resistive and is compatible to different substrate, such as paper, press cloth, and metal [84,85].

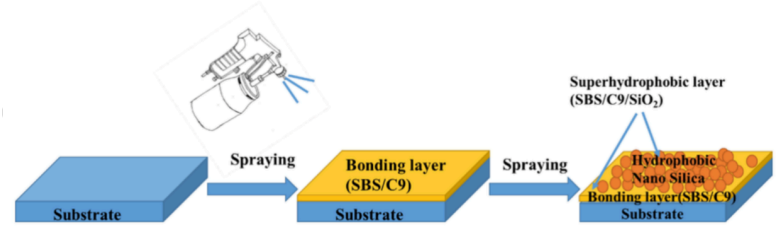

Figure 14. Schematic diagram of the preparation of SBS/C9-SiO_2 coatings on the substrate. Images adapted from prior work [84]

4.2.4. Polyacrylate/SiO_2/Graphene oxide composite

The sp^2 hybrid single-layer-thick graphene is promising in novel water-repellent and anticorrosion material. Xiao and his team combined acrylate copolymer, SiO_2 nanoparticles (SiO_2NPs), and graphene oxide (GO) sheets performing as a barrier against corrosion. SiO_2NPs, together with GO sheets, formed a nanostructure on the surface of the coating (as Fig. 15 shown), providing a high roughness and hence hardness, durability, and superhydrophobicity. In the experient, the modified SiO_2NPs were prepared through a one-pot sol-gel process; the acrylate copolymer was synthesized through radical polymerization [86].

DOI: 10.54254/2755-2721/2026.KA29339

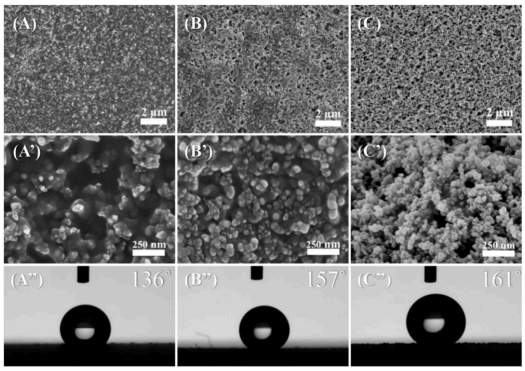

Figure 15. SEM images at different magnifications and WCAs of acrylate copolymer/0.15-SiO2 NPs coating (A, A', A'') acrylate copolymer/0.25-SiO2 NPs coating (B, B', B''), and acrylate copolymer/0.35-SiO2 NPs coating (C, C', C''). Images adapted from prior work [86]

4.3. Application

Driven by increasing regulatory and environmental pressures, non-fluorinated coatings are being adopted in textiles, food packaging, and automotive applications. Recent developments demonstrate that these materials can meet essential performance requirements such as water resistance, surface durability, and material compatibility, offering viable alternatives to traditional fluorinated systems.

In the domains of apparel and home textiles, achieving durable water-repellent properties without reliance on fluorinated compounds is most frequently accomplished using polymer systems based on hydrocarbon and silicone. Hadhri et al. (2025) demonstrate that octylsilane-modified, amino-functional polymers can yield very high static water contact angles on both cotton (130°) and polyester (145°) substrates, while maintaining hydrophobicity across multiple laundering cycles, with approximately 80% of the original contact angle preserved [87]. In recent years, the U.S. Fire Service has initiated the integration of PFAS-free durable water repellents into firefighter turnout gear, representing a substantial step forward in the adoption of non-fluorinated protective textiles [88]. Both PFAS-based and non-PFAS outer shell materials have been subjected to simulated occupational exposures, followed by comprehensive evaluations of their water repellency, durability, thermal protection performance, and surface chemical properties [88]. According to Mazumder et al. (2023)'s findings, although water-repellent properties of non-PFAS outer shell materials are largely maintained, their resistance to hydrocarbon-based contaminants such as diesel is diminished, which may increase the risk of flammability [88]. Nevertheless, the non-fluorinated systems demonstrate thermal and mechanical performance, as well as water resistance, broadly comparable to their PFAS-containing counterparts, highlighting the potential of fluorine-free DWR finishes for use in high-performance textile applications [88].

In the development of fiber-based food service ware, fluorine-free barrier technologies are progressively transitioning toward the use of biobased or hybrid coating systems. Ahuja et al. (2024) developed a crosslinked shellac coating that imparts excellent water and grease resistance, with Cobb60 values below 25 g/m2, indicating low water absorption over 60 seconds of exposure, and a Kit rating of 9 out of 12, which reflects high resistance to penetration by low surface tension oils in standardized contact tests [89]. The coating adheres tightly to molded fiber substrates, remains intact under flexing, and meets both food-contact safety and compost ability standards [89]. Similarly, Zhang et al. (2023) proposed a fully bio-based cellulose nanofibril (CNF) coating for molded pulp containers, achieving a maximum Kit rating (12/12) and improved hot water resistance [90]. The dense fibril network reduced oil penetration while preserving recyclability and biodegradability [90].

DOI: 10.54254/2755-2721/2026.KA29339

Both approaches demonstrate that natural polymer coatings such as shellac and CNF can meet key barrier requirements for single-use packaging while complying with FDA and EU food-contact regulations.

Non-fluorinated hydrophobic coatings are increasingly applied to automotive glass, mirrors, and sensor covers to improve water repellency, visibility, and surface cleanliness. Shahzadi et al. (2021) synthesized a transparent polyacrylate-based coating embedded with TiO_2 nanoparticles [91]. The coating exhibited a high-water contact angle of 135° and maintained over 97% visible light transmittance. It also showed enhanced scratch resistance and self-cleaning behavior under natural conditions, making it suitable for windshields and external optical components [91]. Zhang et al. (2024) introduced a fluorine-free superhydrophobic coating prepared from silica nanoparticles and a silica sol matrix [92]. Applied to automotive glass, the surface achieved a contact angle exceeding 160° with a sliding angle below 5° [92]. The coating retained transparency and durability under water impact and abrasion tests, supporting its use in dynamic environments [92]. These results demonstrate that fluorine-free coatings can meet both optical and functional requirements for automotive applications, especially in rain-shedding, anti-fogging, and easy-cleaning functions.

5. Comparison between different non-fluorinated DWR coatings and future outlook

5.1. Hydrocarbon-based non-fluorinated DWR coatings

Hydrocarbon-based durable water repellents have garnered increasing attention as sustainable alternatives to fluorinated compounds. Unlike fluorinated substances such as perfluoroalkyl substances, hydrocarbon-based systems reduce surface energy and impart hydrophobicity through the incorporation of long-chain alkyl groups, which are typically introduced via fatty acids, waxes, or hydrocarbon-bearing polymers [11]. These DWRs are valued for their environmental compatibility and cost-effectiveness, making them attractive for applications in consumer textiles and food-contact materials [11,93]. However, they face substantial challenges in achieving comparable durability, hydrostatic resistance, and service life when subjected to repeated laundering, mechanical abrasion, and extended environmental exposure [94]. Additionally, most hydrocarbon-based coatings exhibit weaker interfacial adhesion to textile fibers and are generally unable to repel oils, a limitation resulting from their relatively higher surface energy compared to fluorinated systems [94]. As a result, recent research efforts have turned toward the development of next-generation hydrocarbon-based DWRs, including long-chain alkyl acrylate copolymers and alkyl polysaccharide esters (APS), with the goal of enhancing functional performance while preserving environmental advantages [27].

Alkyl polysaccharide esters are biopolymer-based DWRs synthesized by esterifying long-chain fatty acids such as stearic acid (C_{18}) onto polysaccharide backbones including chitosan and starch. These materials represent a promising route to combine hydrophobicity with biodegradability. In a recent study, a stearoyl-modified chitosan coating applied to textile substrates achieved a static water contact angle of 133°, which remained above 118° after ten laundering cycles although the repellency decreased thereafter [95]. Furthermore, the same coating exhibited over 70 percent mass loss within 30 days under industrial composting conditions, demonstrating enhanced environmental degradability [95]. Despite these promising features, both APS and long-chain acrylate-based DWRs generally underperform when compared to fluorinated finishes in key metrics. For instance, typical C_6 to C_8 PFAS-based systems maintain water contact angles above 120° even after 90 home laundering cycles, and routinely exhibit hydrostatic breakthrough pressures exceeding 90

DOI: 10.54254/2755-2721/2026.KA29339

centimeters of water [96,97]. These benchmarks remain difficult to achieve with current hydrocarbon-based alternatives.

Long-chain alkyl acrylate copolymers, which consist of monomers such as stearyl acrylate (C18) or hexadecyl acrylate (C_{16}) copolymerized with hydrophilic or cross linkable co-monomers, have shown improved wash resistance compared to traditional paraffin- or wax-based treatments. Studies have confirmed that such copolymers can deliver static contact angles exceeding 120° and exhibit modest durability after multiple laundering cycles [98]. To further enhance their performance, researchers have proposed strategies such as increasing molecular crosslinking density to stabilize the film network, and introducing nanostructured surface roughness through silica or clay nanoparticles to create hierarchical topographies that promote water repellency by invoking Cassie–Baxter-type wetting regimes [99]. However, standardized testing using ISO and AATCC protocols remains essential to accurately evaluate wash fastness, hydrostatic pressure resistance, and abrasion durability for these next-generation hydrocarbon-based coatings [96].

In summary, although long-chain alkyl acrylate copolymers and APS-based systems offer distinct environmental and safety advantages, neither fully replicates the superior mechanical and fluid barrier performance of fluorinated DWRs. Their future development will rely on molecular engineering, performance benchmarking, and lifecycle assessment to address existing limitations while supporting global transitions away from PFAS-based technologies.

5.2. Silicone-based non-fluorinated DWR coatings

5.2.1. Silicon-containing DWRs (silane and siloxane sealers)

A wide range of durable water repellents currently available for commercial applications are silicone-based. These products are commonly marketed in emulsion form and may be either water- or solvent-based. When applied to textiles, they typically undergo padding, drying, and curing processes, with the curing step being feasible even at room temperature. To enhance oil, soil, and water repellence, silicone formulations are sometimes combined with perfluoroalkyl (PFA) chains; however, this approach introduces fluorine-containing residues upon decomposition.

Among non-fluorinated DWRs, two major categories derived from silicone molecules are silane sealers and siloxane sealers. Both types penetrate into the substrate to impart long-lasting water repellence and anti-freezing properties, thereby protecting building structures from thaw damage, chloride intrusion, microbial growth, and efflorescence. Sharing a characteristic silicon–oxygen–silicon backbone as the core of their polymeric chains, these materials are generally referred to under the generic name “silicone.” As penetrating-type sealers, both silane and siloxane exhibit several similarities: they maintain high substrate breathability, allowing water vapor to diffuse outward while preventing external liquid water penetration; and they generally preserve, or only slightly alter (e.g., imparting a glossy finish), the appearance of the treated substrate. Despite these commonalities, their performance characteristics differ considerably [100].

5.2.1.1. Mechanism and operating conditions

Silane sealers, when applied to substrates such as concrete, react with calcium hydroxide within the alkaline matrix to form a hydrophobic resin. A noteworthy limitation is that the substrate must be alkaline; therefore, silane sealers are ineffective on non-alkaline building materials such as natural stone, wood, or clay-based blocks [101].

DOI: 10.54254/2755-2721/2026.KA29339

In contrast, siloxane sealers do not depend on the pH of the substrate. Instead, they undergo chemical reactions with moisture from either the atmosphere or the substrate itself, forming a water-repellent resin. This feature renders siloxane sealers more versatile across a wider range of materials commonly employed in modern construction [102].

5.2.1.2. Key features and performance

Beyond differences in reaction pathways, the molecular size of the two sealers plays a critical role in their practical performance.

Silane sealers, composed of relatively small molecules, are able to penetrate deeply into dense substrates such as precast or poured-in-place concrete. This deep penetration enhances their resistance to abrasion and weathering. However, their small molecular size also leads to high volatility, which results in considerable material loss during application and curing. To compensate, higher solid content must be used, increasing cost and inefficiency [101].

Siloxane sealers, by contrast, consist of larger molecules. Their lower volatility reduces waste during application, lowers production costs, and improves stability on moderately dense substrates [102,103].

5.2.2. R-7000 soft hydro guard

In 2012, Dow Corning introduced an environmentally friendly silicone-based textile finish known as DWR-7000 Soft Hydro Guard. Unlike conventional DWRs, this finish is notable for its exceptional softness in addition to comfort and performance benefits. Its water repellency and durability on cellulosic textiles and blends have been demonstrated to be comparable to those of fluorinated DWRs, such as fluorochemical C6-type finishes. Importantly, DWR-7000 Soft Hydro Guard achieves these properties without relying on fluorine, solvents, or alkylphenol ethoxylates (APEOs), which are widely used in traditional DWRs. Consequently, this finish avoids issues of toxicity and bioaccumulation, thereby reducing risks to soil-dwelling organisms and agricultural crops exposed to its decomposition products [104].

5.3. Bio-based non-fluorinated DWR coatings

5.3.1. Categories of bio-based material

Compared with hydrocarbon materials, bio-based materials refer to the materials that are wholly or partly derived from biological resources such as plants, animals, microorganisms, and marine biomass. From the perspective of the component, bio-based materials can be divided into four types: wax, fatty acid, natural polymer, and carbohydrate [105].

Waxes always represent the substance that is a plastic solid at ambient temperature, and turns into a viscous liquid at elevated temperature. In nature, waxes are one of the most ubiquitous substances that increase the hydrophobicity of plants, animals, and even minerals. Waxes involve a myriad of chemicals, encompassing hydrocarbons, fatty acids, and so on, which are all long chains of carbon, so they can’t form a strong interaction with water molecules. However, this type of material can’t possess high durability alone. As a result, waxes will always be combined with nanoparticles and polymers to increase their thermal and adhesive stability.

Fatty acids refer to the carboxylic acids with long aliphatic chains, which are either saturated or have a double bond. In general, when the chain is longer, its surface energy will be lower, possessing a stronger hydrophobicity, such as Lignoceric acid (C24), compared with stearic acid (C18).

DOI: 10.54254/2755-2721/2026.KA29339

Moreover, saturated fatty acid has a higher melting point compared with unsaturated fatty acids because saturated fatty acids can form a more regular sequence, which can increase the contact area between each other and decrease the interaction with water molecules further. Fatty acid plays an essential role in the biological reactions of the animal's body. Because of its high percentage of lipids, it helps animals to store energy and sustain their life activities. In addition, fatty acids can be found in various plant seeds. For instance, behenic acid, a carboxylic acid with a 20-carbon chain, can be extracted from the seed of the peanut and flax.

Natural polymer consists of repeated structural units extracted from plants, and they have gained great interest because of their renewable property and abundance. However, although polymers show excellent water repellency, the difficulty of fabricating them uniformly and rapidly is a challenge to manufacturing them at a low cost. Compared with other bio-based materials, these natural polymers lack the antibacterial property due to the absence of an activated group, such as aromatic phenol and carboxylic acid. In fact, these polymers will be consumed by the bacteria.

Carbohydrates are ubiquitous in nature, and among carbohydrates, polysaccharides are relatively representative materials in the field of hydrophobicity. Even if the majority of polysaccharides are hydrophilic, the role they play on the surface is adhesion, which means they can bind textile fabrics and hydrophobic molecules densely. Given that the hydroxy groups are on their structure, the hydrophobic molecules can adhere to the surface persistently, promoting the durability and also flexibility of bio-based material [106].

5.3.2. RUCO-DRY BIO CGR

As the first superhydrophobic DWR entirely based on natural waste -- by-products that accumulate during the processing of cereal grains in the food industry, RUCO-DRY BIO CGR indicates a terrific hydrophobic and stain-resistant property in the experiment. Firstly, RUCO-DRY BIO CGR's spray rating is 100, which means its water repellency reaches the highest level compared with other DWRs. Secondly, it has a wonderful durability, according to Rudolf Duraner, RUCO-DRY BIO CGR can sustain its hydrophobicity after less than 30 times washing. Even though its water repellency disappears, its property can recover after drying or ironing. Thirdly, RUCO-DRY BIO CGR possesses a distinguished stain-resistance, which can be illustrated from the test of coffee and juice. Last but not least, consisting of 90% bio carbon, RUCO-DRY BIO CGR is environmentally friendly and easy to degrade outdoors [107].

5.3.3. DOWSIL™ IE-9100

DOWSIL™ IE-9100 Emulsion is an organo-silicone hybrid emulsion with a high superhydrophobic performance in the field of bio-based materials. Although it has only 81% bio-based components, it was announced that it "rivals the performance of fluorinated DWR". In comparison with other materials, its durability can sustain excellent water repellency after more than 20 washes. In addition, DOWSIL IE-9100 is easy to dilute and combine with other ingredients to tailor performance to application requirements, including synthetic, natural, and blended fiber fabrics [108].

5.3.4. Comparison

Both DWRs are state-of-the-art in the bio-based material, and RUCO-DRY BIO CGR has an obviously stronger hydrophobic property than DOWSIL IE-9100. Nevertheless, both materials lack enough data to support their concrete property in distinct aspects. For instance, RUCO-DRY BIO

DOI: 10.54254/2755-2721/2026.KA29339

CGR doesn't illustrate good performance in the oil repellency in the report, and DOWSIL IE-9100 has limited data to prove it can "rival the system of fluorinated DWR". Moreover, RUCO-DRY BIO CGR must involve a booster to ensure its durability, which increases the difficulty of manufacturing this type of DWR. After all, both DWR have a fabulous hydrophobic property in comparison with fluorinated DWR, and relatively high biodegradable property. Even though they have several drawbacks, they are a better choice to apply in daily life under the contemporary restriction of fluorinated DWR.

5.4. Nanoparticle-based non-fluorinated DWR coatings

Nanoparticle-based non-fluorinated durable water repellent coatings are an advanced technological solution that combines micro/nanoscale surface roughness—achieved through nanoparticles—with low surface energy, which is regulated by fluorine-free modifiers. This integrated design makes them a strong competitor to traditional fluorinated coatings and even surpasses some non-fluorinated options, such as pure silicone or hydrocarbon-based systems, in terms of balancing water resistance and environmental sustainability [109].

These coatings typically employ inorganic nanoparticles (e.g., silica, zinc oxide, titanium dioxide) or organic nanoparticles (e.g., polymer microspheres) as structural components. Thanks to their small size (10–100 nm) and high surface area, these particles can self-assemble into dense, hierarchical structures that mimic the natural water-repellent surfaces of lotus leaves [110]. Beyond these conventional materials, two emerging systems—cellulose nanocrystal (CNC) coatings and metal-organic framework (MOF)-modified nanoparticle coatings—have drawn significant attention due to their unique performance characteristics, positioning them at the forefront of non-fluorinated DWR research.

CNC-based coatings use rod-like nanoparticles sourced from renewable plant materials such as wood pulp or cotton. These particles typically measure 5–20 nm in diameter and 100–500 nm in length. Since their surface contains many hydrophilic hydroxyl groups (Figure 5-1), they must be treated with fluorine-free agents like octadecyl isocyanate or stearic acid to introduce hydrophobic alkyl chains. Once modified, the CNCs can form rough, hierarchical coatings on fabrics such as cotton or polyester through processes like dip-coating or spray-coating. In terms of performance, these coatings often achieve water contact angles (WCAs) between 140° and 155°, and can repel 5 μL water droplets at tilt angles below 15° [111]. A major advantage is their biodegradability—they break down naturally in soil within 3–6 months, avoiding the environmental persistence associated with synthetic nanoparticles. However, CNC coatings also have drawbacks: their rod-like structure is susceptible to damage under abrasion, leading to a 40% loss of roughness after 100 cycles, and residual hydroxyl groups can absorb moisture in highly humid conditions (RH > 80%), reducing the WCA by up to 30% after three months outdoors [111]. On a practical level, CNC coatings are relatively inexpensive (around $5–10/kg) and compatible with roll-to-roll manufacturing, making them suitable for eco-friendly disposable textiles or biodegradable packaging.

DOI: 10.54254/2755-2721/2026.KA29339

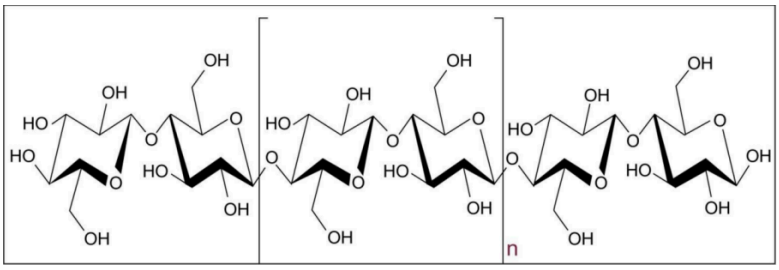

Figure 16. The chemical structure of cellulose, which is a linear polymer made up of β-D-glucopyranose units covalently linked with (1–4) glycosidic bonds. Images adapted from prior work [109]

In comparison, MOF-modified nanoparticle coatings make use of porous crystalline structures composed of metal ions (e.g., Zn^{2+}, Cu^{2+}) and organic linkers. With adjustable pore sizes (1–10 nm) and high specific surface areas (over 1000 m^2/g), MOFs are typically applied as coatings around inorganic nanoparticles or assembled into 20–50 nm clusters [112]. This design improves air entrapment and, when modified with low-energy substances such as trimethyl silane, brings surface energy down to 21–23 mN/m. MOF-based coatings achieve WCAs of 150–160° with low roll-off angles (<10°) and high breakthrough pressure (1.2–1.5 kPa)—surpassing pure silica coatings by 50–80%—while maintaining sound chemical stability [112]. However, MOF synthesis remains costly ($20–30 per kg) due to stringent reaction conditions, and particle aggregation during large-scale coating often requires dispersants that may compromise performance. These constraints currently restrict MOF-based coatings to high-value sectors, including professional outdoor and marine gear.

To further boost water repellency, all types of nanoparticle coatings—conventional, CNC, or MOF-based—can be treated with fluorine-free modifiers such as silane coupling agents, long-chain alcohols, or natural waxes. These substances lower surface energy via covalent or non-covalent bonding, enabling superhydrophobicity with WCAs above 150° and better self-cleaning performance, even when their surface energy remains slightly higher than that of fluorinated analogues [113] .

Nevertheless, issues concerning durability, breakthrough pressure, and service life persist. Mechanical stresses—including washing and abrasion—damage the nanoparticle layers; for instance, silica-based coatings on cotton may lose 40% of their water repellency after five launderings [114]. Porous coatings are also prone to water penetration under high pressure or extended wet conditions [115]. UV exposure, oxidation, and microbial activity further shorten functional durability, generally limiting outdoor service life to 6–12 months—less than the 2–3 years typical of fluorinated coatings.

Future progress will likely concentrate on mitigating these shortcomings through surface engineering with cross linkable groups to strengthen adhesion and abrasion resistance [116], blending nanoparticles with flexible polymers such as PDMS or polyurethane to improve toughness, and devising more scalable application methods. Such innovations are crucial for broadening the adoption of non-fluorinated DWR coatings across textiles, construction, and medical devices.

6. Conclusion

In conclusion, this review has underscored the pressing necessity to transition from environmentally hazardous fluorinated DWRs towards sustainable alternatives, drawing upon an analysis of wettability and hydrophobicity fundamentals, bioinspired models from natural surfaces, and the four principal categories of non-fluorinated coatings. Although hydrocarbon-based, silicon-based, bio-

DOI: 10.54254/2755-2721/2026.KA29339

derived, and nanoparticle-based systems exhibit considerable potential in terms of hydrophobicity and ecological safety, issues pertaining to durability, oil resistance, and commercial viability remain unresolved. Moving forward, advancements in this field will hinge on the integration of biomimetic principles and sophisticated synthesis techniques to develop coatings that optimally reconcile performance, sustainability, and scalability.

Acknowledgement

Zicheng Tang, Yuerong Tian, Chenyu Zhang, and Dechen Feng contributed equally to this work and should be considered co-first authors.

References

[1] Guo, Z., & Yang, F. (2018). Surfaces and interfaces of biomimetic superhydrophobic materials. Wiley-VCH.
[2] Trager, R. (2019, August 27). A persistent perfluorinated problem.
[3] Shurson, G. C. (2025). The Alarming Effects of Per- and Polyfluoroalkyl Substances (PFAS) on One Health and Interconnections with Food-Producing Animals in Circular and Sustainable Agri-Food Systems. Sustainability, 17(15), 6957. https: //doi.org/10.3390/su17156957
[4] Yu, R., Yu, H., Yang, Y., & Singh, S. (2025). A Global Overview of Per- and Polyfluoroalkyl Substance Regulatory Strategies and Their Environmental Impact. Toxics, 13(4), 251. https: //doi.org/10.3390/toxics13040251
[5] Taves, D. R. (1968). Evidence that there are Two Forms of Fluoride in Human Serum. Nature, 217(5133), 1050–1051. https: //doi.org/10.1038/2171050b0
[6] Biodegradation of Fluorinated Alkyl Substances. (n.d.). SpringerLink. Retrieved July 26, 2025, from https: //link.springer.com/chapter/10.1007/978-1-4419-6880-7_3
[7] Perfluoroalkyl and polyfluoroalkyl substances in the environment: terminology, classification, and origins. (n.d.). PubMed. Retrieved July 26, 2025, from https: //pubmed.ncbi.nlm.nih.gov/21793199/
[8] Wang, Z., Cousins, I. T., Scheringer, M., & Hungerbühler, K. (2013). Fluorinated alternatives to long-chain perfluoroalkyl carboxylic acids (PFCAs), perfluoroalkane sulfonic acids (PFSAs) and their potential precursors. Environ. Int., 60, 242–248. https: //doi.org/10.1016/j.envint.2013.08.021
[9] Hill, P. J., Taylor, M., Goswami, P., & Blackburn, R. S. (2017). Substitution of PFAS chemistry in outdoor apparel and the impact on repellency performance. Chemosphere, 181, 500–507. https: //doi.org/10.1016/j.chemosphere.2017.04.122
[10] Non-fluorinated sprayable fabric finish for durable and comfortable superhydrophobic textiles. (2021). Prog. Org. Coat., 157, 106319. https: //doi.org/10.1016/j.porgcoat.2021.106319
[11] Holmquist, H., Schellenberger, S., Van Der Veen, I., Peters, G. M., Leonards, P. E. G., & Cousins, I. T. (2016). Properties, performance and associated hazards of state-of-the-art durable water repellent (DWR) chemistry for textile finishing. Environ. Int., 91, 251–264. https: //doi.org/10.1016/j.envint.2016.02.035
[12] Williams, J. T. (2017). Waterproof and Water Repellent Textiles and Clothing. Woodhead Publishing.
[13] Hu, J., Nie, K., Meng, Q., & Zheng, G. (2008). Multifunction Finishing Liquids Containing Dendrimers and the Application of the Liquids in Textile Finishing. US20080282480A1. Retrieved July 24, 2025, from https: //patents.google.com/patent/US20080282480A1/en
[14] Namligoz, E. S., Bahtiyari, M. I., Hosaf, E., & Coban, S. (2009). Performance Comparison of New (Dendrimer, Nanoproduct) and Conventional Water, Oil and Stain Repellentss. Fibres Text. East. Eur., 17(5), 76. Retrieved July 24, 2025, from http: //yadda.icm.edu.pl/baztech/element/bwmeta1.element.baztech-0577a093-fe20-4fa8-9197-42bd39fed6d8
[15] Outdoor Participation Trends Report 2024. (n.d.). American Trails. Retrieved July 26, 2025, from https: //www.americantrails.org/resources/outdoor-participation-trends-report-2024
[16] Clothing. The portable environment. (1985). In Applied Ergonomics (p. 305). Elsevier BV. https: //doi.org/10.1016/0003-6870(85)90128-0
[17] Functional finishes to improve the comfort and protection of apparel. (2013). In Advances in the Dyeing and Finishing of Technical Textiles (pp. 258–279). Woodhead Publishing. https: //doi.org/10.1533/9780857097613.2.258
[18] Principle of Textile Testing by J.E Booth. (n.d.). Scribd. Retrieved July 26, 2025, from https: //www.scribd.com/document/614443873/Principle-of-Textile-Testing-by-J-E-Booth-Textilestudycenter-com

DOI: 10.54254/2755-2721/2026.KA29339

[19] Functional Clothing Design: From Sportswear to Space Suits. (n.d.). College of Design. Retrieved July 26, 2025, from https: //design.umn.edu/wearable-technology-lab/research/functional-clothing-design
[20] Essentials of Sea Survival. (n.d.). ResearchGate. Retrieved July 26, 2025, from https: //www.researchgate.net/publication/270283180_Essentials_of_Sea_Survival
[21] Improving moisture management in apparel. (2011). In Improving Comfort in Clothing (pp. 182–215). Woodhead Publishing. https: //doi.org/10.1533/9780857090645.2.182
[22] Blum, A., et al. (2015). The Madrid Statement on Poly- and Perfluoroalkyl Substances (PFASs). Environ. Health Perspect., 123(5), A107–A111. https: //doi.org/10.1289/ehp.1509934
[23] Schellenberger, S., Hill, P. J., Levenstam, O., Gillgard, P., Cousins, I. T., Taylor, M., & Blackburn, R. S. (2019). Highly fluorinated chemicals in functional textiles can be replaced by re-evaluating liquid repellency and end-user requirements. Journal of Cleaner Production, 217, 134–143. https: //doi.org/10.1016/j.jclepro.2019.01.160
[24] Schellenberger, S., Gillgard, P., Stare, A., Hanning, A., Levenstam, O., Roos, S., & Cousins, I. T. (2018). Facing the rain after the phase out: Performance evaluation of alternative fluorinated and non-fluorinated durable water repellents for outdoor fabrics. Chemosphere, 193, 675–684. https: //doi.org/10.1016/j.chemosphere.2017.11.027
[25] Williams, J. (2018). Waterproof and water repellent textiles and clothing. The Textile Institute; Duxford, United Kingdom; Cambridge, Ma, United States.
[26] Sharif, R., Mohsin, M., Haji Ghulam Qutab, Saleem, F., Bano, S., Nasir, R., & Ahtesham Wahlah. (2023). Durable water and oil repellents along with green chemistries: an overview. Chemical Papers, 77(7), 3547–3560. https: //doi.org/10.1007/s11696-023-02763-x
[27] Chen, S., Lai, J., Du, Y., & Hong, Z. (2025). Review on Non-fluorinated Durable Water Repellent Alternatives for Textile and Fabric Coatings. Science and Technology of Engineering Chemistry and Environmental Protection, 1(11). https: //doi.org/10.61173/s8tf6n88
[28] Josyula, T., Malla, L. K., Thomas, T. M., Kalichetty, S. S., Mahapatra, P. S., & Pattamatta, A. (2024). Fundamentals and Applications of Surface Wetting. Langmuir. https: //doi.org/10.1021/acs.langmuir.3c03339
[29] Huhtamäki, T., Tian, X., Korhonen, J. T., & Ras, R. H. A. (2018). Surface-wetting characterization using contact-angle measurements. Nature Protocols, 13(7), 1521–1538. https: //doi.org/10.1038/s41596-018-0003-z
[30] Young, T. (1805). An Essay on the Cohesion of Fluids. Philosophical Transactions of the Royal Society of London, 95, 65–87. https: //doi.org/10.2307/107159
[31] Harvie, D. J. E. (2024). Contact-angle hysteresis on rough surfaces: mechanical energy balance framework. Journal of Fluid Mechanics, 986. https: //doi.org/10.1017/jfm.2024.317
[32] Law, K.-Y. (2021). Contact Angle Hysteresis on Smooth/Flat and Rough Surfaces. Interpretation, Mechanism, and Origin. Accounts of Materials Research. https: //doi.org/10.1021/accountsmr.1c00051
[33] Furmidge, C. G. L. (1962). Studies at phase interfaces. I. The sliding of liquid drops on solid surfaces and a theory for spray retention. Journal of Colloid Science, 17(4), 309–324. https: //doi.org/10.1016/0095-8522(62)90011-9
[34] Sun, Q., Chen, Y.-N., & Liu, Y.-Z. (2025). Wetting Transition from Wenzel to Cassie States: Thermodynamic Analysis. Materials, 18(3), 543. https: //doi.org/10.3390/ma18030543
[35] Khojasteh, D., Kazerooni, M., Salarian, S., & Kamali, R. (2016). Droplet impact on superhydrophobic surfaces: A review of recent developments. Journal of Industrial and Engineering Chemistry, 42, 1–14. https: //doi.org/10.1016/j.jiec.2016.07.027
[36] Sotoudeh, F., Mousavi, S. M., Karimi, N., Lee, B. J., Abolfazli-Esfahani, J., & Manshadi, M. K. D. (2023). Natural and synthetic superhydrophobic surfaces: A review of the fundamentals, structures, and applications. Alexandria Engineering Journal, 68, 587–609. https: //doi.org/10.1016/j.aej.2023.01.058
[37] Wenzel, R. N. (1936). RESISTANCE OF SOLID SURFACES TO WETTING BY WATER. Industrial & Engineering Chemistry, 28(8), 988–994. https: //doi.org/10.1021/ie50320a024
[38] Cassie, A. B. D., & Baxter, S. (1944). Wettability of porous surfaces. Transactions of the Faraday Society, 40, 546. https: //doi.org/10.1039/tf9444000546
[39] Callies, M., & Quéré, D. (2005). On water repellency. Soft Matter, 1(1), 55–61. https: //doi.org/10.1039/B501657F
[40] Stephenson, R. J. Mechanics And Properties Of Matter.
[41] Ghoufi, A., Malfreyt, P., & Tildesley, D. J. (2016). Computer modelling of the surface tension of the gas–liquid and liquid–liquid interface. Chem. Soc. Rev., 45(5), 1387–1409. https: //doi.org/10.1039/C5CS00736D
[42] Koopal, L. K. (2012). Wetting of Solid Surfaces: Fundamentals and Charge effects. Adv. Colloid Interface Sci., 179–182, 29–42. https: //doi.org/10.1016/j.cis.2012.06.009
[43] Clint, J. H. (2001). Adhesion and components of solid surface energies. Curr. Opin. Colloid Interface Sci., 6(1), 28–33. https: //doi.org/10.1016/S1359-0294(00)00084-4
[44] Spreading Coefficients for Wettability. (n.d.). Fundamentals of Fluid Flow in Porous Media. Retrieved July 25, 2025, from https: //perminc.com/resources/fundamentals-of-fluid-flow-in-porous-media/chapter-2-the-porous-

DOI: 10.54254/2755-2721/2026.KA29339

medium/multi-phase-saturated-rock-properties/wettability/spreading-coefficients/
[45] Moody, V., & Needles, H. L. (2004). Stain blockers and fluorochemicals. In Elsevier eBooks (pp. 177–191). https: //doi.org/10.1016/b978-188420799-0.50017-8
[46] Abo-Basha, S. S., Nassar, K. M., & Mohamed, R. A. (2024). Antistatic textiles: current status and future outlook. Deleted Journal, 3(2). https: //doi.org/10.55554/2785-9649.1033
[47] Libretexts. (2023, February 13). 9: diffusion. Chemistry LibreTexts. https: //chem.libretexts.org/Bookshelves/Physical_and_Theoretical_Chemistry_Textbook_Maps/Supplemental_Modules_(Physical_and_Theoretical_Chemistry)/Kinetics/09%3A_Diffusion
[48] Zhang, G., Wang, D., Yan, J., Xiao, Y., Gu, W., & Zang, C. (2019). Study on the photocatalytic and Antibacterial Properties of TIO2 Nanoparticles-Coated Cotton Fabrics. Materials, 12(12), 2010. https: //doi.org/10.3390/ma12122010
[49] Liang, L., Luo, Z., Mao, Q., et al. Preparation of hydrophobic fabrics and effect of fluorine.
[50] Myronyuk, O., Vanagas, E., Rodin, A. M., & Wesolowski, M. (2024). Estimation of the Structure of Hydrophobic Surfaces Using the Cassie–Baxter Equation. Materials, 17(17), 4322. https: //doi.org/10.3390/ma17174322
[51] Ge, H., Liu, Y., & Liu, F. (2023). Up to Date Review of Nature-Inspired Superhydrophobic Textiles: Fabrication and Applications. Materials, 16(21), 7015. https: //doi.org/10.3390/ma16217015
[52] Mail, M., Koch, K., Speck, T., Megill, W., & Gorb, S. N. (2023). Biomimetics on the micro- and nanoscale – The 25th anniversary of the lotus effect. Beilstein Journal of Nanotechnology, 14, 850–856. https: //doi.org/10.3762/bjnano.14.69
[53] Wang, Y., Li, J., Song, H., Wang, F., Su, X., Zhang, D., & Xu, J. (2025). Biomimetic Superhydrophobic Surfaces: From Nature to Application. Materials, 18(12), 2772. https: //doi.org/10.3390/ma18122772
[54] Southall, E. J., & Sims, D. W. (2003). Shark skin: a function in feeding. Proceedings of the Royal Society B Biological Sciences, 270(suppl_1). https: //doi.org/10.1098/rsbl.2003.0006
[55] Gabler-Smith, M. K., Wainwright, D. K., Wong, G. A., & Lauder, G. V. (2021). Dermal Denticle Diversity in sharks: Novel Patterns on the Interbranchial skin. Integrative Organismal Biology, 3(1). https: //doi.org/10.1093/iob/obab034
[56] T. B. H. Schroeder, J. Houghtaling, B. D. Wilts, and M. Mayer, “It’s Not a Bug, It’s a Feature: Functional Materials in Insects, ” Adv. Mater., vol. 30, no. 19, p. 1705322, 2018, doi: 10.1002/adma.201705322.
[57] W.-K. Kuo, J.-J. Hsu, C.-K. Nien, and H. H. Yu, “Moth-Eye-Inspired Biophotonic Surfaces with Antireflective and Hydrophobic Characteristics, ” ACS Appl. Mater. Interfaces, vol. 8, no. 46, pp. 32021–32030, Nov. 2016, doi: 10.1021/acsami.6b10960.
[58] Stadlmayr, S., Peter, K., Millesi, F., Rad, A., Wolf, S., Mero, S., Zehl, M., Mentler, A., Gusenbauer, C., Konnerth, J., Schniepp, H. C., Lichtenegger, H., Naghilou, A., & Radtke, C. (2023). Comparative Analysis of Various Spider Silks in Regard to Nerve Regeneration: Material Properties and Schwann Cell Response. Advanced Healthcare Materials, 13(8). https: //doi.org/10.1002/adhm.202302968.
[59] Wang, Q.; McArdle, P.; Wang, S. L.; Wilmington, R. L.; Xing, Z.; Greenwood, A.; Cotten, M. L.; Qazilbash, M. M.; Schniepp, H. C. Protein secondary structure in spider silk nanofibrils. Nature Communications 2022, 13 (1). https: //doi.org/10.1038/s41467-022-31883-3.
[60] Šede, M.; Fridmanis, J.; Otikovs, M.; Johansson, J.; Rising, A.; Kronqvist, N.; Jaudzems, K. Solution Structure of tubuliform spidroin N-Terminal domain and implications for pH dependent dimerization. Frontiers in Molecular Biosciences 2022, 9. https: //doi.org/10.3389/fmolb.2022.936887.
[61] Kronqvist, N.; Otikovs, M.; Chmyrov, V.; Chen, G.; Andersson, M.; Nordling, K.; Landreh, M.; Sarr, M.; Jörnvall, H.; Wennmalm, S.; Widengren, J.; Meng, Q.; Rising, A.; Otzen, D.; Knight, S. D.; Jaudzems, K.; Johansson, J. Sequential pH-driven dimerization and stabilization of the N-terminal domain enables rapid spider silk formation. Nature Communications 2014, 5 (1). https: //doi.org/10.1038/ncomms4254.
[62] Su, I.; Buehler, M. J. Nanomechanics of silk: the fundamentals of a strong, tough and versatile material. Nanotechnology 2016, 27 (30), 302001. https: //doi.org/10.1088/0957-4484/27/30/302001.
[63] Su, Y.; Shi, S.; Wang, C.; Wang, Z.; Li, P.; Zhang, S.; Fei, B.; Yang, Z.; Hu, J. Spider silk-inspired tough materials: Multi-pathway synthesis, advanced processing, and functional applications. Nano Today 2024, 55, 102188. https: //doi.org/10.1016/j.nantod.2024.102188.
[64] Song, W.; Mu, Z.; Zhang, Z.; Wang, Y.; Hu, H.; Ma, Z.; Huang, L.; Wang, Z.; Zhang, B.; Li, Y.; Zhang, S.; Li, B.; Zhang, J.; Niu, S.; Han, Z.; Ren, L. Cross-Scale Biological Models of Species for Future Biomimetic Composite Design: A review. Coatings 2021, 11 (11), 1297. https: //doi.org/10.3390/coatings11111297.
[65] Steffen H. and Hans-Jürgen B. (2022) Fluid Interfaces with and without Adsorbed Species under Homogeneous Electric Field

DOI: 10.54254/2755-2721/2026.KA29339

[66] Ghoufi, A. (2025b). Atomistic computing of the solid–fluid surface free energy and tension. Nature Reviews Physics. https: //doi.org/10.1038/s42254-025-00855-z
[67] Tang, Z., Li, H., Hess, D. W., & Breedveld, V. (2016). Effect of chain length on the wetting properties of alkyltrichlorosilane coated cellulose-based paper. Cellulose, 23(2), 1401–1413. https: //doi.org/10.1007/s10570-016-0877-2
[68] Owen, M. J. Why silicones behave funny. In: Biomedical Engineering Desk Reference, National Academic Digital Library of Ethiopia, 2012. https: //www.sciencedirect.com/science/article/abs/pii/B9780080877808001078
[69] Samyn, P., & Rastogi, V. K. (2022). Stabilization of an Aqueous Bio-Based Wax Nano-Emulsion through Encapsulation. Nanomaterials, 12(23), 4329. https: //doi.org/10.3390/nano12234329
[70] Liu, I. C.; Hu, X.; Fei, B.; Lee, C.; Fan, S.; Xin, J. H.; Noor, N. Fluorine-free nanoparticle coatings on cotton fabric: comparing the UV-protective and hydrophobic capabilities of silica vs. silica-ZnO nanostructures. RSC Advances 2024, 14 (7), 4301–4314. https: //doi.org/10.1039/d3ra08835a.
[71] (A) Reaction scheme for the nanoparticle formation and cotton fabric... ResearchGate. https: //www.researchgate.net/figure/A-Reaction-scheme-for-the-nanoparticle-formation-and-cotton-fabric-coating-B_fig1_377842897.
[72] Luo, W.; Li, M. Recent advances in fabrication of durable, transparent, and superhydrophobic surfaces. Nanomaterials 2023, 13 (16), 2359. https: //doi.org/10.3390/nano13162359.
[73] Edwards, N.; Goswami, P. Plasma-based treatments of textiles for water repellency. ResearchGate 2017.
[74] Reema, N.; Khanikar, R. R.; Bailung, H.; Sankaranarayanan, K. Review of the cold atmospheric plasma technology application in food, disinfection, and textiles: A way forward for achieving circular economy. Frontiers in Physics 2022, 10. https: //doi.org/10.3389/fphy.2022.942952.
[75] Ahmed, H. A. M. Plasma treatment in Textile Substrates - a review. ResearchGate 2012.
[76] Asadollahi, S.; Profili, J.; Farzaneh, M.; Stafford, L. Development of Organosilicon-Based Superhydrophobic Coatings through Atmospheric Pressure Plasma Polymerization of HMDSO in Nitrogen Plasma. Materials 2019, 12 (2), 219. https: //doi.org/10.3390/ma12020219.
[77] Fig. 1. Description of the low pressure plasma process. ResearchGate. https: //www.researchgate.net/figure/Description-of-the-low-pressure-plasma-process_fig1_232389108.
[78] Duan, A.; Gu, F.; Jiang, X.; Du, J.; Shao, D.; Xu, C. Washable Superhydrophobic Cotton Fabric with Photothermal Self-Healing Performance Based on Nanocrystal-MXene. ACS Applied Materials & Interfaces 2025. https: //doi.org/10.1021/acsami.4c21715.
[79] Yu, P.; Yu, Z.; Liao, K.; Xia, S.; Li, K.; Chen, J. Preparation of superhydrophobic coatings by saturated fatty acid modification using a one-step spraying method. Applied Surface Science 2025, 162612. https: //doi.org/10.1016/j.apsusc.2025.162612.
[80] Y. Wang et al., “Advances in Sol-Gel-Based Superhydrophobic Coatings for Wood: A Review, ” Int. J. Mol. Sci., vol. 24, no. 11, p. 9675, June 2023, doi: 10.3390/ijms24119675.
[81] M. Shigrekar and V. Amdoskar, “A review on recent progress and techniques used for fabricating superhydrophobic coatings derived from biobased materials, ” RSC Adv., vol. 14, no. 44, pp. 32668–32699, 2024, doi: 10.1039/D4RA04767B.
[82] J. J. Kalmoni, F. L. Heale, C. S. Blackman, I. P. Parkin, and C. J. Carmalt, “A Single-Step Route to Robust and Fluorine-Free Superhydrophobic Coatings via Aerosol-Assisted Chemical Vapor Deposition, ” Langmuir, May 2023, doi: 10.1021/acs.langmuir.3c00554.
[83] “(PDF) Aerosol-assisted delivery of precursors for chemical vapour deposition: Expanding the scope of CVD for materials fabrication, ” ResearchGate, Aug. 2025, doi: 10.1039/c3dt50607j.
[84] N. J. Janowicz et al., “Fluorine-Free Transparent Superhydrophobic Nanocomposite Coatings from Mesoporous Silica, ” Langmuir, vol. 36, no. 45, pp. 13426–13438, Nov. 2020, doi: 10.1021/acs.langmuir.0c01767.
[85] “(PDF) A Simple and Convenient Method for Preparing Fluorine-Free Durable Superhydrophobic Coatings Suitable for Multiple Substrates, ” ResearchGate, Apr. 2025, doi: 10.3390/ma16051771.
[86] P. Xiao, L. Yang, J. Liu, X. Zhang, and D. Chen, “A non-fluorinated superhydrophobic composite coating with excellent anticorrosion and wear-resistant performance, ” Front. Chem., vol. 10, Oct. 2022, doi: 10.3389/fchem.2022.952919.
[87] Hadhri, M., Colleoni, C., Agnese D’Agostino, Erhaim, M., Rosa, R. P., Rosace, G., & Trovato, V. (2025). Eco-Friendly Octylsilane-Modified Amino-Functional Silicone Coatings for a Durable Hybrid Organic–Inorganic Water-Repellent Textile Finish. Polymers, 17(11), 1578–1578. https: //doi.org/10.3390/polym17111578
[88] Mazumder, N.-U.-S., Lu, J., Andrew Stephen Hall, Arash Kasebi, Arjunsing Girase, Masoud, F., Stull, J. O., & R. Bryan Ormond. (2023). Toward the future of firefighter gear: Assessing fluorinated and non-fluorinated outer shells

DOI: 10.54254/2755-2721/2026.KA29339

following simulated on-the-job exposures. Journal of Industrial Textiles, 53. https: //doi.org/10.1177/15280837231217401
[89] Ahuja, A., & Vibhore Kumar Rastogi. (2024). PFAS free, food-grade, water and grease-resistant coating based on crosslinked shellac for molded pulp products. Progress in Organic Coatings, 196, 108734–108734. https: //doi.org/10.1016/j.porgcoat.2024.108734
[90] Zhang, J., & Youngblood, J. P. (2023). Cellulose Nanofibril (CNF)-Coated PFAS-Free, Grease-Resistant All-Bio-Based Molded Pulp Containers for Food Packaging. ACS Applied Polymer Materials, 5(7), 5696–5706. https: //doi.org/10.1021/acsapm.3c00979
[91] Zhang, B., Xue, X., Zhao, L., & Hou, B. (2024). Transparent Superhydrophobic and Self-Cleaning Coating. Polymers, 16(13), 1876–1876. https: //doi.org/10.3390/polym16131876
[92] Shahzadi, P., Gilani, S. R., Rana, B. B., Ghaffar, A., & Munir, A. (2021). Transparent, self-cleaning, scratch resistance and environment friendly coatings for glass substrate and their potential applications in outdoor and automobile industry. Scientific Reports, 11(1). https: //doi.org/10.1038/s41598-021-00230-9
[93] Danish EPA. (2015). Alternatives to perfluoroalkyl and polyfluoroalkyl substances (PFAS) in textiles. Environmental Project No. 1707.
[94] Schellenberger, S., et al. (2018). Release of side-chain fluorinated polymer-containing microplastic fibers from functional textiles during washing and first estimates of perfluoroalkyl acid emissions. Environmental Science & Technology, 53(24), 14329–14338. DOI: 10.1021/acs.est.9b04165
[95] Lee, M., et al. (2022). Hydrophobically modified chitosan via stearoyl esterification for sustainable water-repellent coatings. Carbohydrate Polymers, 286, 119385. DOI: 10.1016/j.carbpol.2022.119385
[96] Xu, L., et al. (2023). Comparative performance of PFAS and non-PFAS DWR finishes in firefighter protective clothing. Textile Research Journal, 93(5), 812–824. DOI: 10.1177/00405175221123174
[97] Fiedler, D., et al. (2019). Evaluation of water and oil repellency and durability of environmentally friendly textile coatings. Journal of Industrial Textiles, 49(6), 718–735. DOI: 10.1177/1528083718785022
[98] Shohbuke, H., et al. (2021). Effects of alkyl acrylate monomer content on the performance of waterborne polyurethane acrylate for textile finishing. Progress in Organic Coatings, 159, 106415. DOI: 10.1016/j.porgcoat.2021.106415
[99] Jiang, Y., et al. (2022). Superhydrophobic nanostructured coatings using silica nanoparticles for fluorine-free durable water repellency. Textile Research Journal, 92(13–14), 2747–2760. DOI: 10.1177/00405175211035149
[100]H. Ziya Özek, “Silicone-based water repellents, ” in Waterproof and Water Repellent Textiles and Clothing, Elsevier, 2018, pp. 153–189. doi: 10.1016/B978-0-08-101212-3.00026-5.
[101]M. Roos, F. König, S. Stadtmüller, and B. Weyershausen, “Evolution of Silicone Based Water Repellents for Modern Building Protection”.
[102]“Hydrophobicity, Hydrophilicity and Silanes, ” ResearchGate, Aug. 2025, Available: https: //www.researchgate.net/publication/272494216_Hydrophobicity_Hydrophilicity_and_Silanes
[103]“Creating water-repellent effects on wood by treatment with silanes.”Available: https: //www.degruyterbrill.com/document/doi/10.1515/HF.2006.008/html
[104]“Dow Corning® DWR-7000 Soft Hydro Guard Water Repellent for ...” Available: https: //www.yumpu.com/en/document/view/7284588/dow-corningr-dwr-7000-soft-hydro-guard-water-repellent-for-
[105]Fleetwood, S. K.; Bell, S.; Jetter, R.; Foster, E. J. Plant-based, aqueous, water-repellent sprays for coating textiles. Soft Matter 2023, 19 (36), 7020–7032. https: //doi.org/10.1039/d3sm00720k.
[106]Jerič, P.; Likozar, B.; Novak, U. Biobased Hydrophobic Solutions for Natural Textiles—Moving beyond PFAS. Journal of Composites Science 2025, 9 (2), 81. https: //doi.org/10.3390/jcs9020081.
[107]RUDOLF GROUP. RUCO®-DRY BIO CGR: Back to Nature and Beyond Fluorine-free. https: //www.rudolf-duraner.com.tr/fileadmin/user_upload/rudolf_germany/landingpages/leaflet_ruco_dry_bio_cgr_en.pdf.
[108]Report, D. Dow introduces durable water repellent technology DOWSILTM IE-9100. TexSPACE Today. https: //www.texspacetoday.com/dow-introduces-dowsil-ie-9100/.
[109]Wang, K., Shen, Y., Duan, M., Wu, T., Zhao, J., & Wang, J. (2023). Non-fluorinated durable water repellent and stain resistant coating. Applied and Computational Engineering, 7(1), 438–452. https: //doi.org/10.54254/2755-2721/7/20230394
[110]Subhan, M., Choudhury, K., & Neogi, N. (2021). Advances with Molecular Nanomaterials in Industrial Manufacturing Applications. Nanomanufacturing, 1(2), 75–97. https: //doi.org/10.3390/nanomanufacturing1020008
[111]George J, Sabapathi SN. Cellulose nanocrystals: synthesis, functional properties, and applications. Nanotechnol Sci Appl. 2015 Nov 4; 8: 45-54. doi: 10.2147/NSA.S64386. PMID: 26604715; PMCID: PMC4639556.
[112]Jiang, S., Zhang, Z., Wang, D., Wen, Y., Peng, N., & Shang, W. (2021). ZIF-8-based micro-arc oxidation composite coatings enhanced the corrosion resistance and superhydrophobicity of a Mg alloy. Journal of Magnesium and

DOI: 10.54254/2755-2721/2026.KA29339

Alloys, 11(4), 1367–1380. https: //doi.org/10.1016/j.jma.2021.07.027
[113]Sullivan, A., Duan, X., & Yang, J. (2022). Development of a hybrid anti-icing coating with superhydrophobic and electrothermal properties. Science Talks, 4, 100076. https: //doi.org/10.1016/j.sctalk.2022.100076
[114]Pipatchanchai, T., & Srikulkit, K. (2007). Hydrophobicity modification of woven cotton fabric by hydrophobic fumed silica coating. Journal of Sol-Gel Science and Technology, 44(2), 119–123. https: //doi.org/10.1007/s10971-007-1609-8
[115]Xing, D., Zhang, Y., Hu, J., & Yao, L. (2020). Highly Hydrophobic and Self-Cleaning Heat-Treated Larix spp. Prepared by TiO2 and ZnO Particles onto Wood Surface. Coatings, 10(10), 986. https: //doi.org/10.3390/coatings10100986
[116]Huan, X., Shi, K., Yan, J., Lin, S., Li, Y., Jia, X., & Yang, X. (2020). High performance epoxy composites prepared using recycled short carbon fiber with enhanced dispersibility and interfacial bonding through polydopamine surface-modification. Composites Part B Engineering, 193, 107987. https: //doi.org/10.1016/j.compositesb.2020.107987